Are the extremely red AGB stars hiding a close companion?

Flavia Dell'Agli - INAF Observatory of Rome

In collaboration with : F. D'Antona, A. Garcia-Hernandez, M. Groenewegen, D. Kamath, E. Marini, L. Mattsson, M. Tailo, P. Ventura

Studing the AGB dust production

Why carbon stars?

C-stars provides the most relevant contribution to the present-day dust enrichment in sub-solar metallicity environments

Understanding the evolution and dust formation of carbon stars in the LMC with a look at the *JWST*

E. Marini[1,2], F. Dell'Agli[2], M. A. T. Groenewegen[5], D. A. García–Hernández[3,4], L. Mattsson[6], D. Kamath[7], P. Ventura[2], F. D'Antona[2], M. Tailo[8]

Marini + 2021, A&A, 647, 69

SAGE-SPEC in the LMC: ~140 IRS spectra of carbon stars (5-35 micron wavelength coverage)

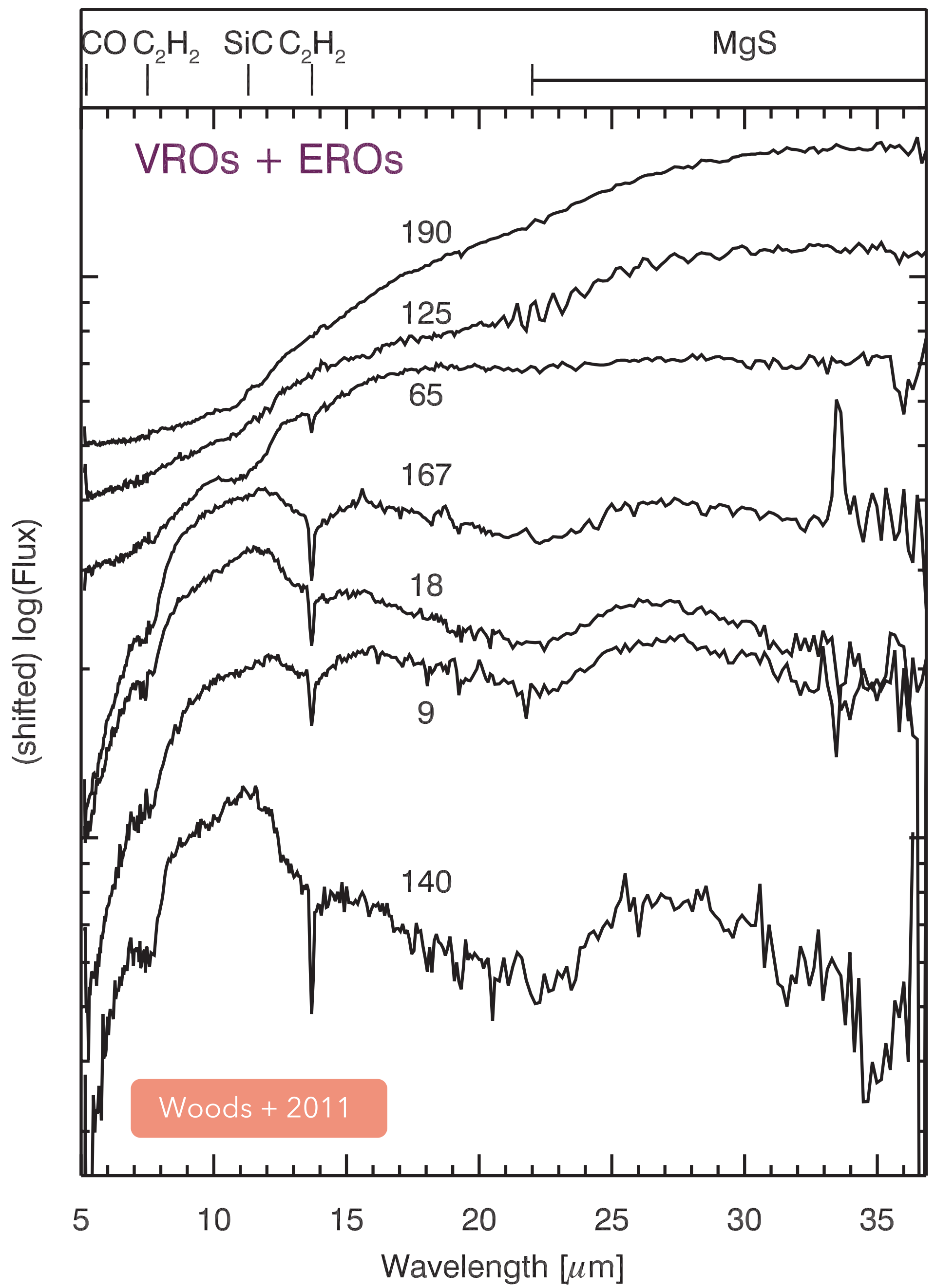

Figure 6. Spectra of the VRO and ERO carbon-rich AGB stars.

Understanding the evolution and dust formation of carbon stars in the LMC with a look at the *JWST*

E. Marini[1,2], F. Dell'Agli[2], M. A. T. Groenewegen[5], D. A. García–Hernández[3,4],
L. Mattsson[6], D. Kamath[7], P. Ventura[2], F. D'Antona[2], M. Tailo[8]

Marini + 2021, A&A, 647, 69

SAGE-SPEC in the LMC: ~140 IRS spectra of carbon stars (5-35 micron wavelength coverage)

Characterization of each source through the comparison with our theoretical models

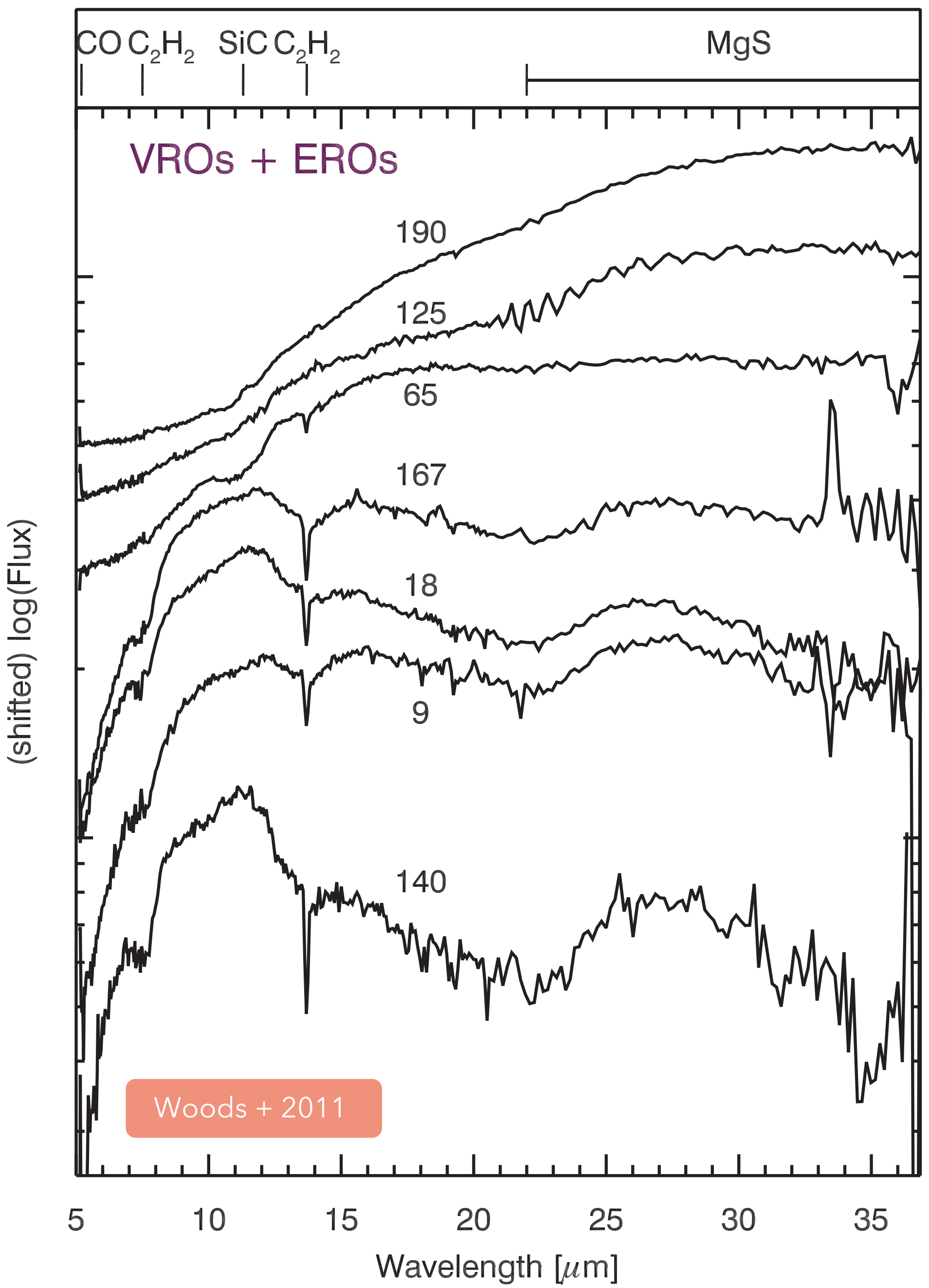

Figure 6. Spectra of the VRO and ERO carbon-rich AGB stars.

Understanding the evolution and dust formation of carbon stars in the LMC with a look at the *JWST*

E. Marini[1,2], F. Dell'Agli[2], M. A. T. Groenewegen[5], D. A. García–Hernández[3,4], L. Mattsson[6], D. Kamath[7], P. Ventura[2], F. D'Antona[2], M. Tailo[8]

Marini + 2021, A&A, 647, 69

- SAGE-SPEC in the LMC: ~140 IRS spectra of carbon stars (5-35 micron wavelength coverage)
- Characterization of each source through the comparison with our theoretical models
- Investigation of the MIRI@JWST filters and diagrams most suitable for the characterization of the carbon AGB sample

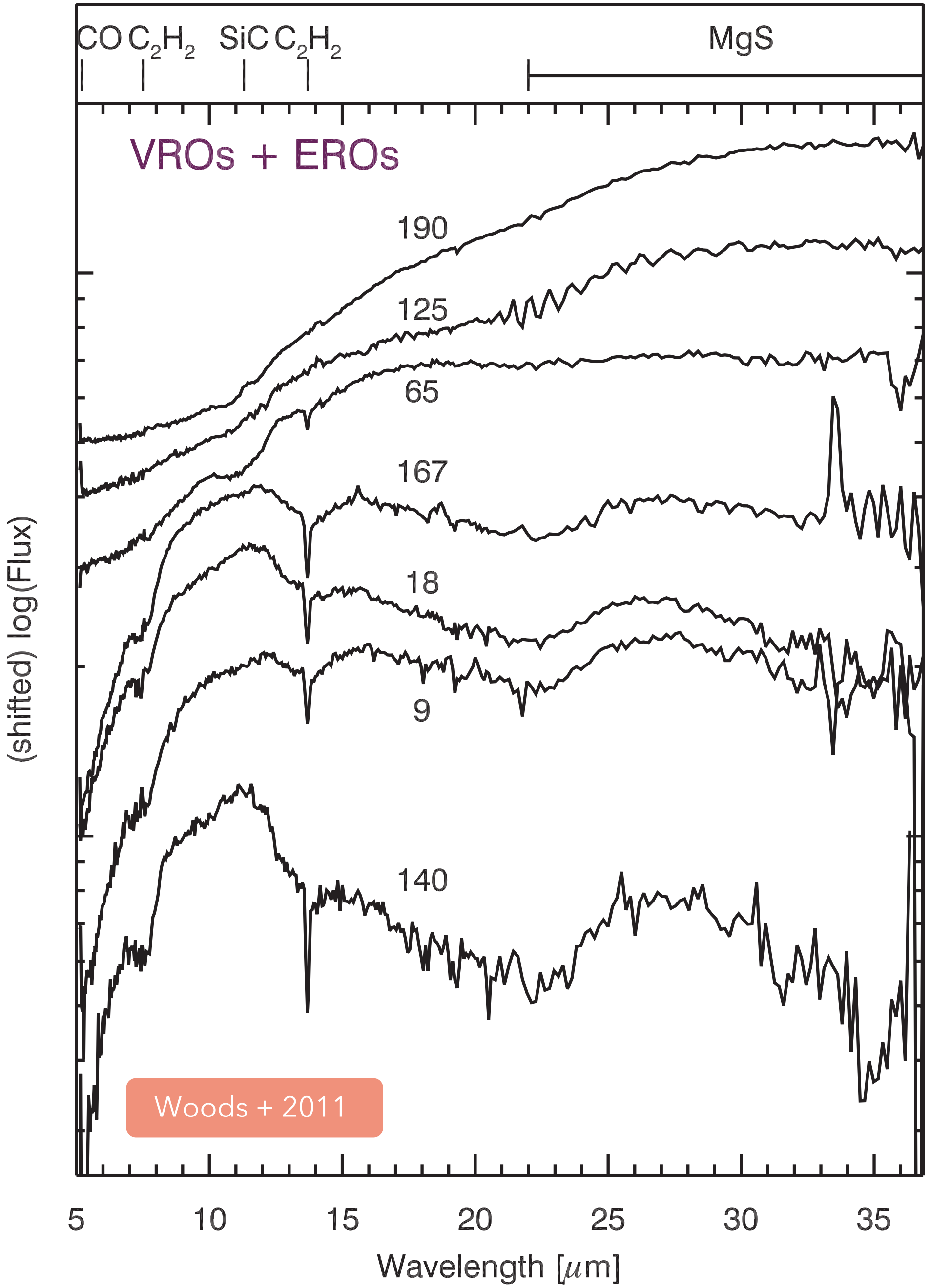

Figure 6. Spectra of the VRO and ERO carbon-rich AGB stars.

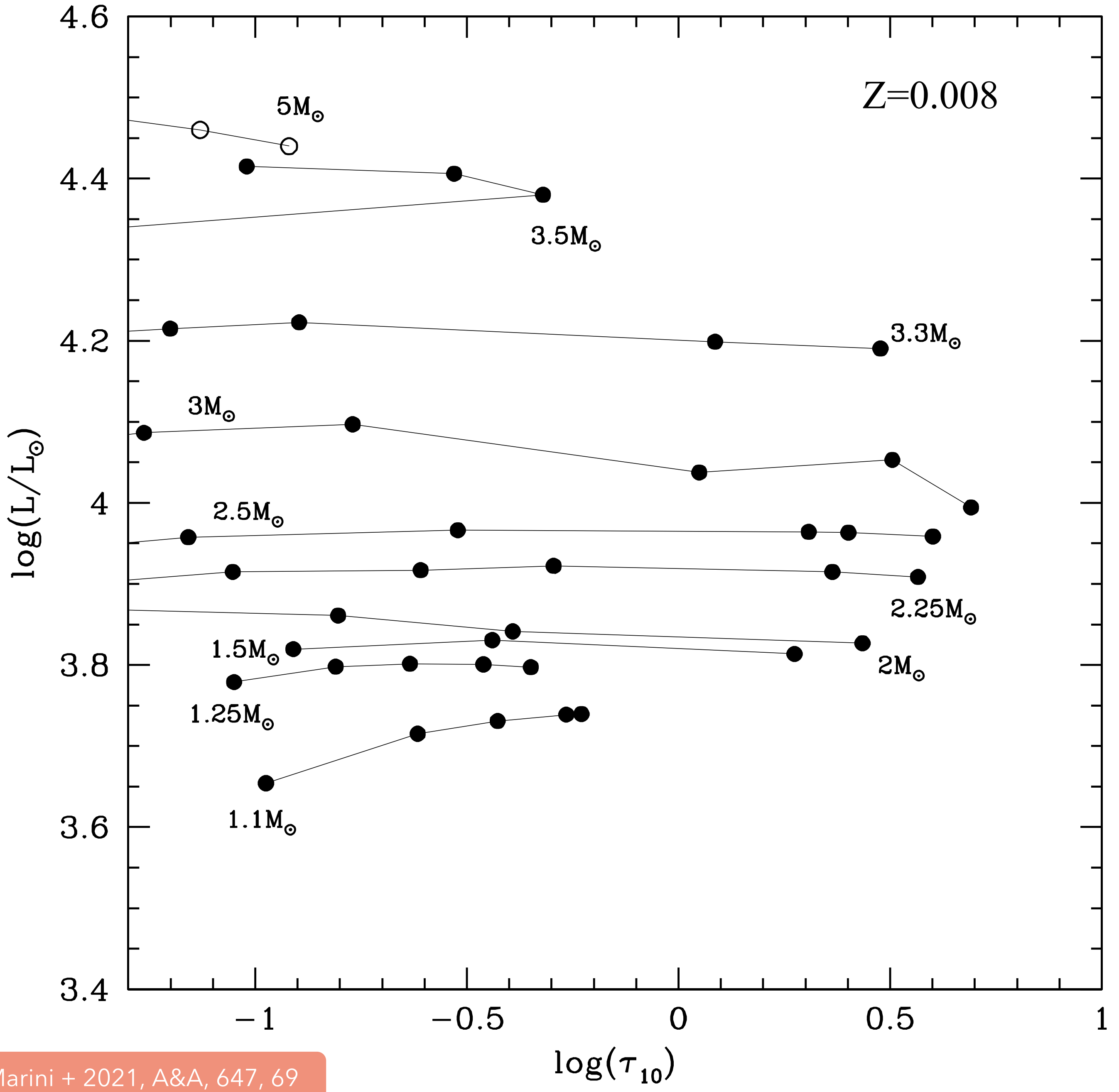

Marini + 2021, A&A, 647, 69

AGB+dust evolutionary tracks from the ATON code (e.g. Ventura+2014)

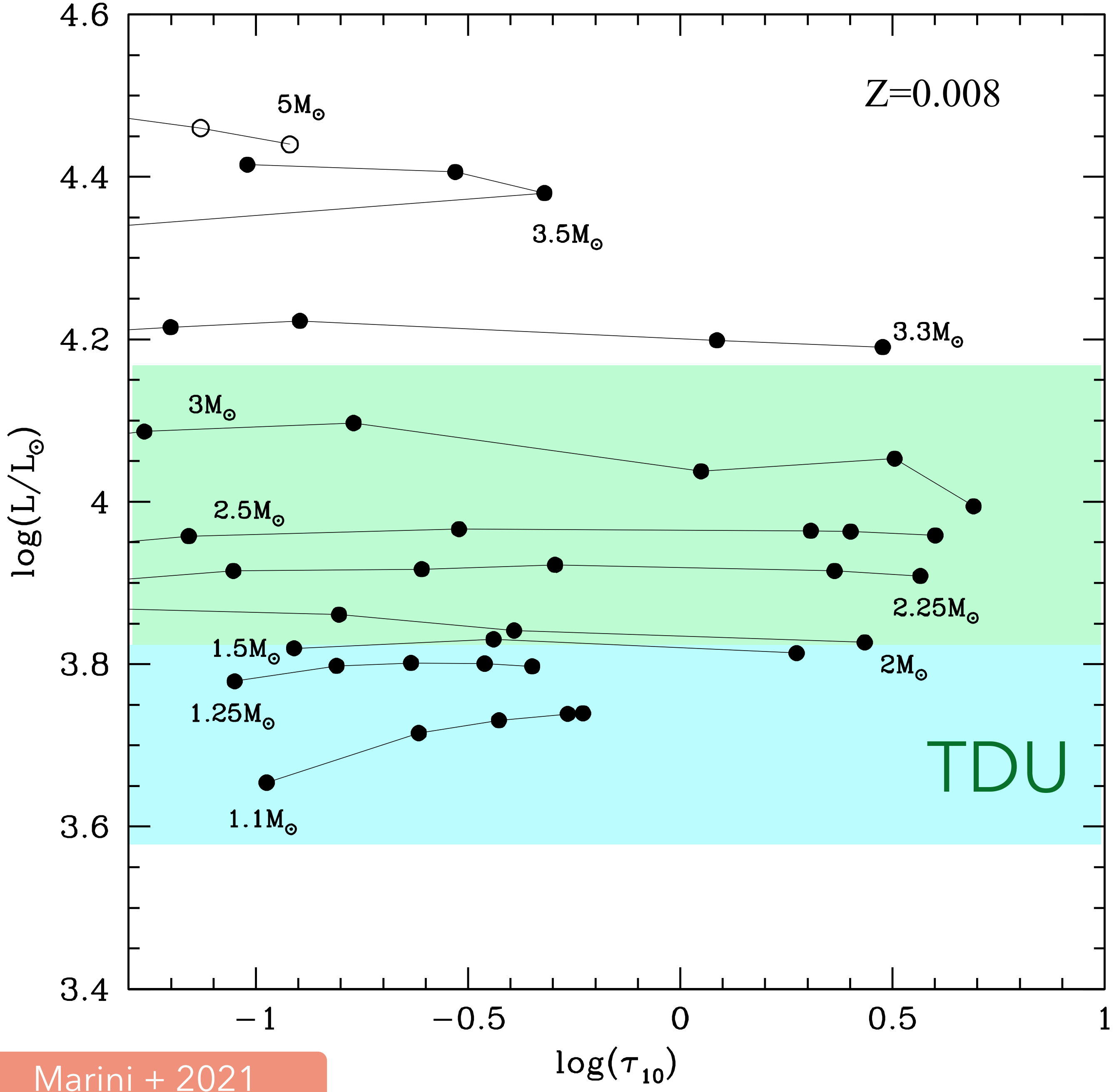

Marini + 2021

AGB+dust evolutionary tracks from the ATON code (e.g. Ventura+2014)

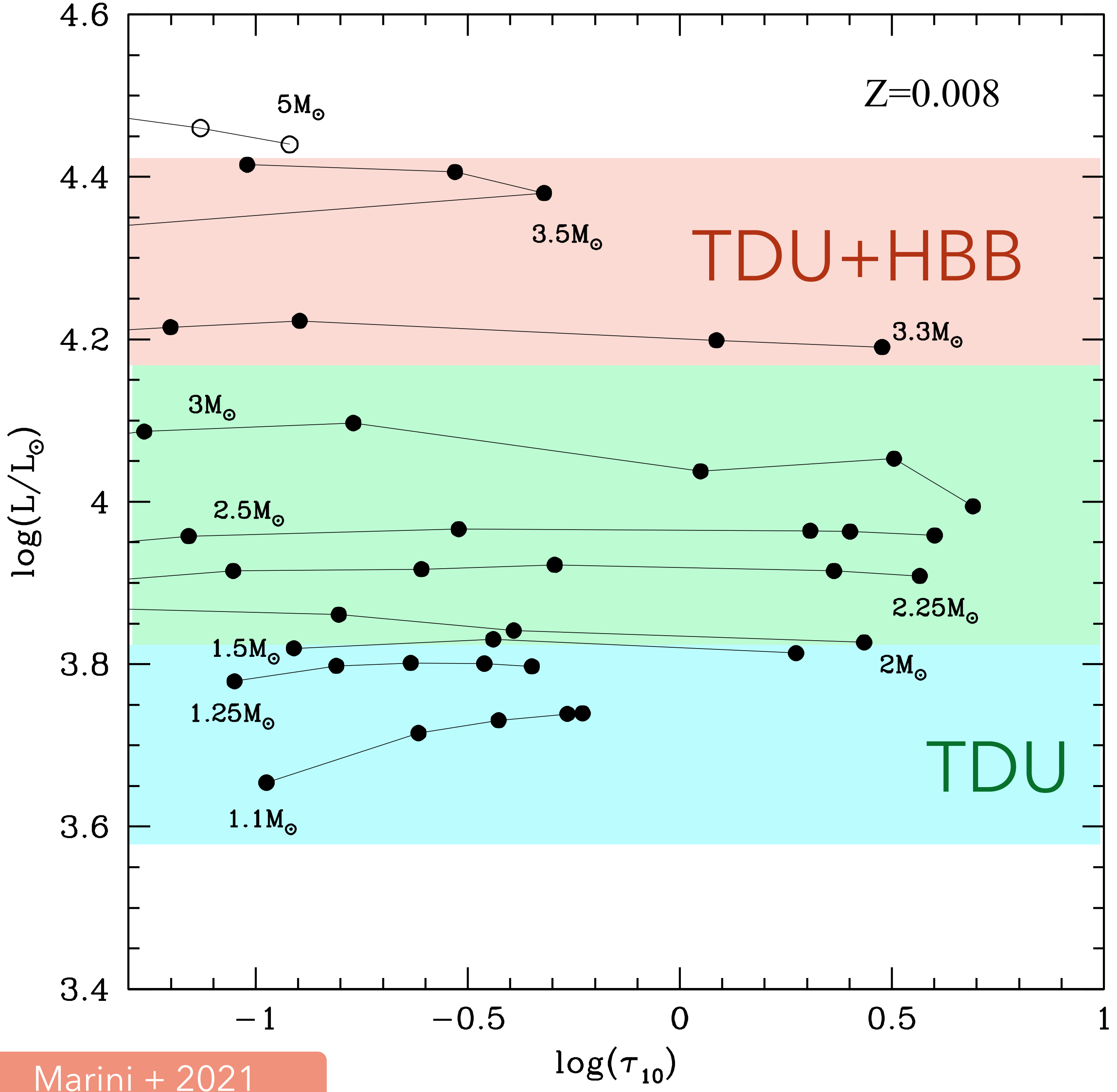

Marini + 2021

AGB+dust evolutionary tracks from the ATON code (e.g. Ventura+2014)

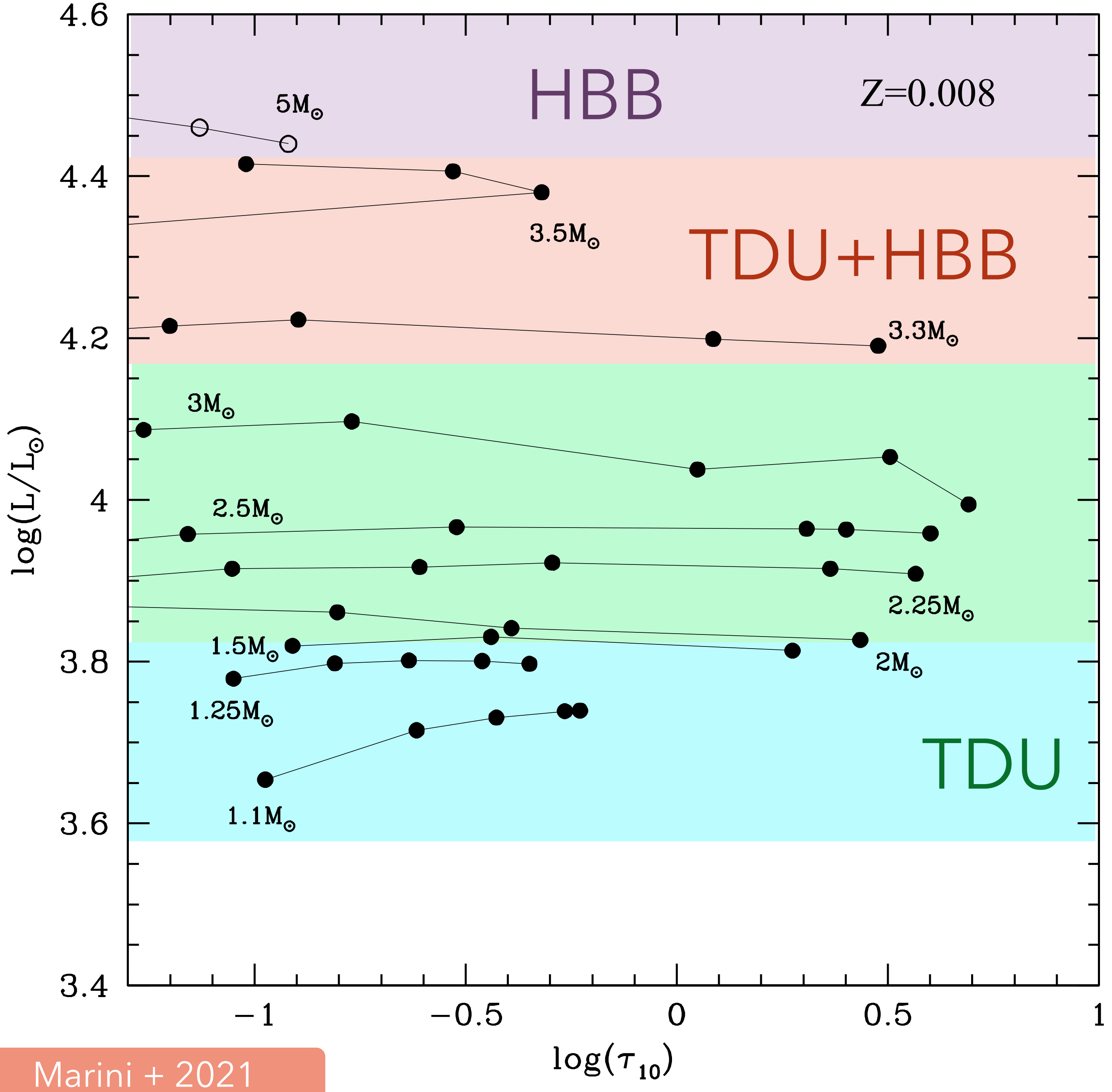

AGB+dust evolutionary tracks from the ATON code (e.g. Ventura+2014)

Marini + 2021

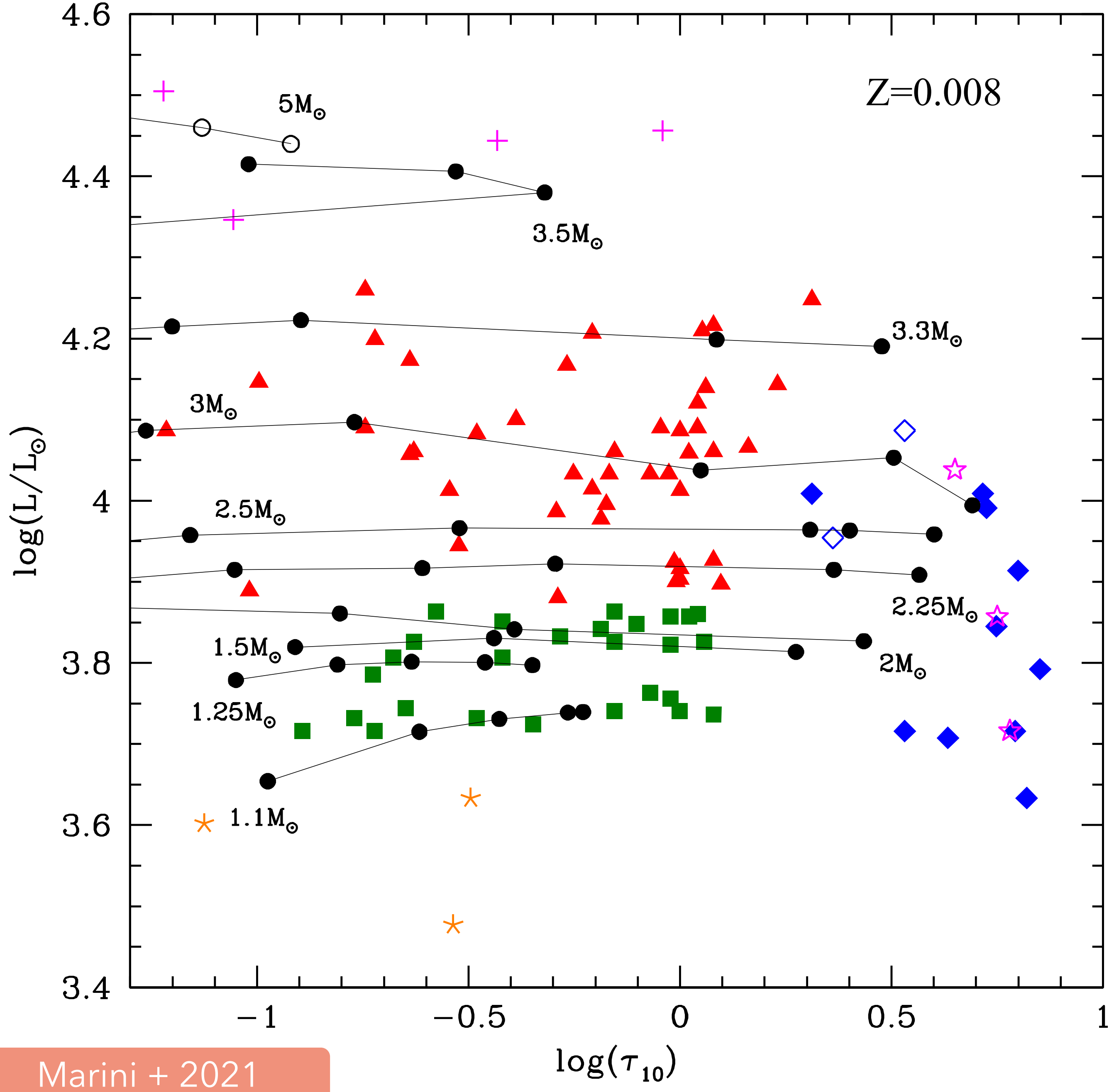

AGB+dust evolutionary tracks from the ATON code (e.g. Ventura+2014)

Marini + 2021

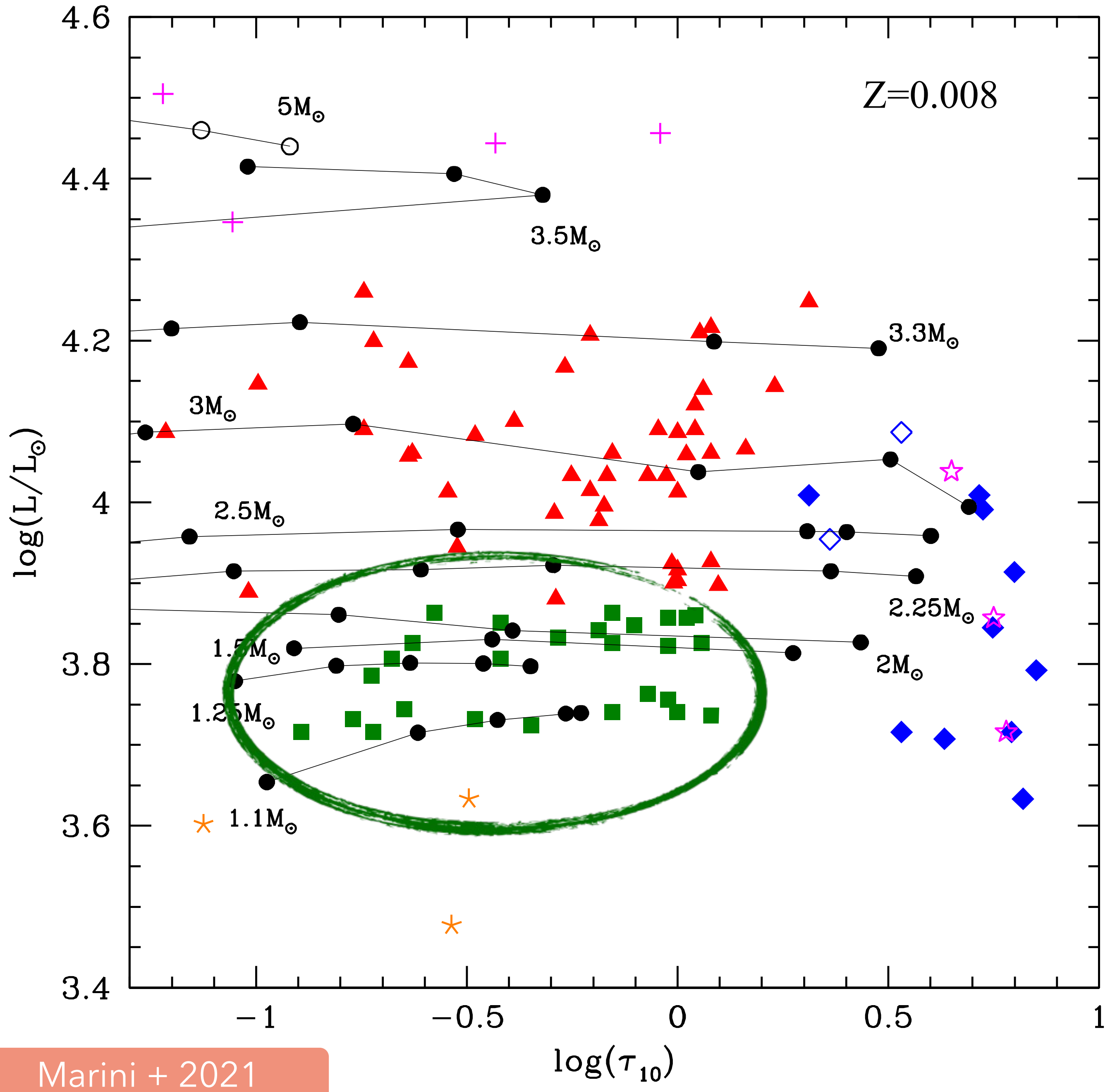

Marini + 2021

AGB+dust evolutionary tracks from the ATON code (e.g. Ventura+2014)

L < 7500 Lsun, ≤2 Msun, formed earlier than 1 Gyr ago.

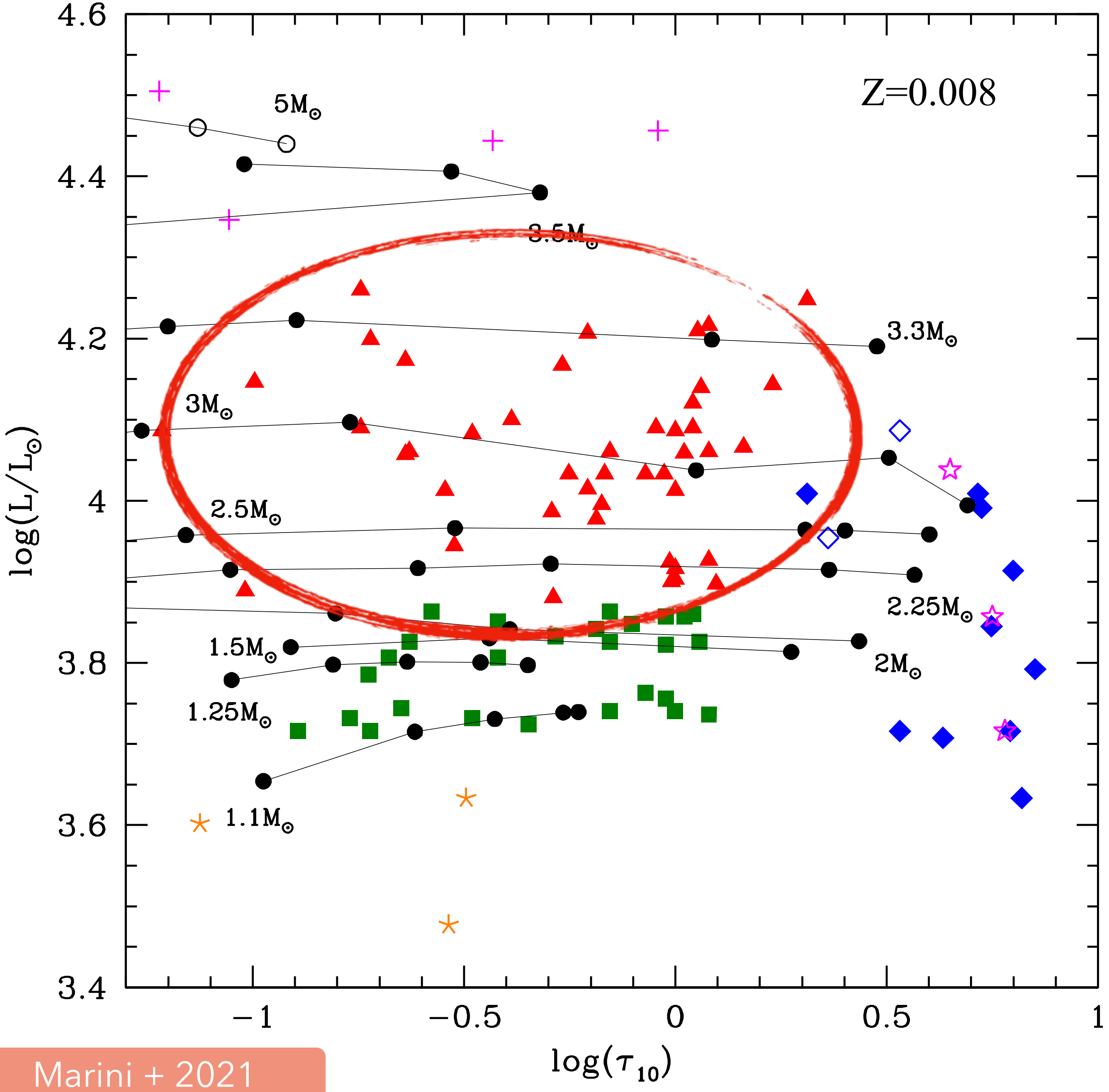

Marini + 2021

AGB+dust evolutionary tracks from the ATON code (e.g. Ventura+2014)

L < 7500 Lsun, <2 Msun, formed earlier than 1 Gyr ago.

Stars younger than 1Gyr, M>2Msun

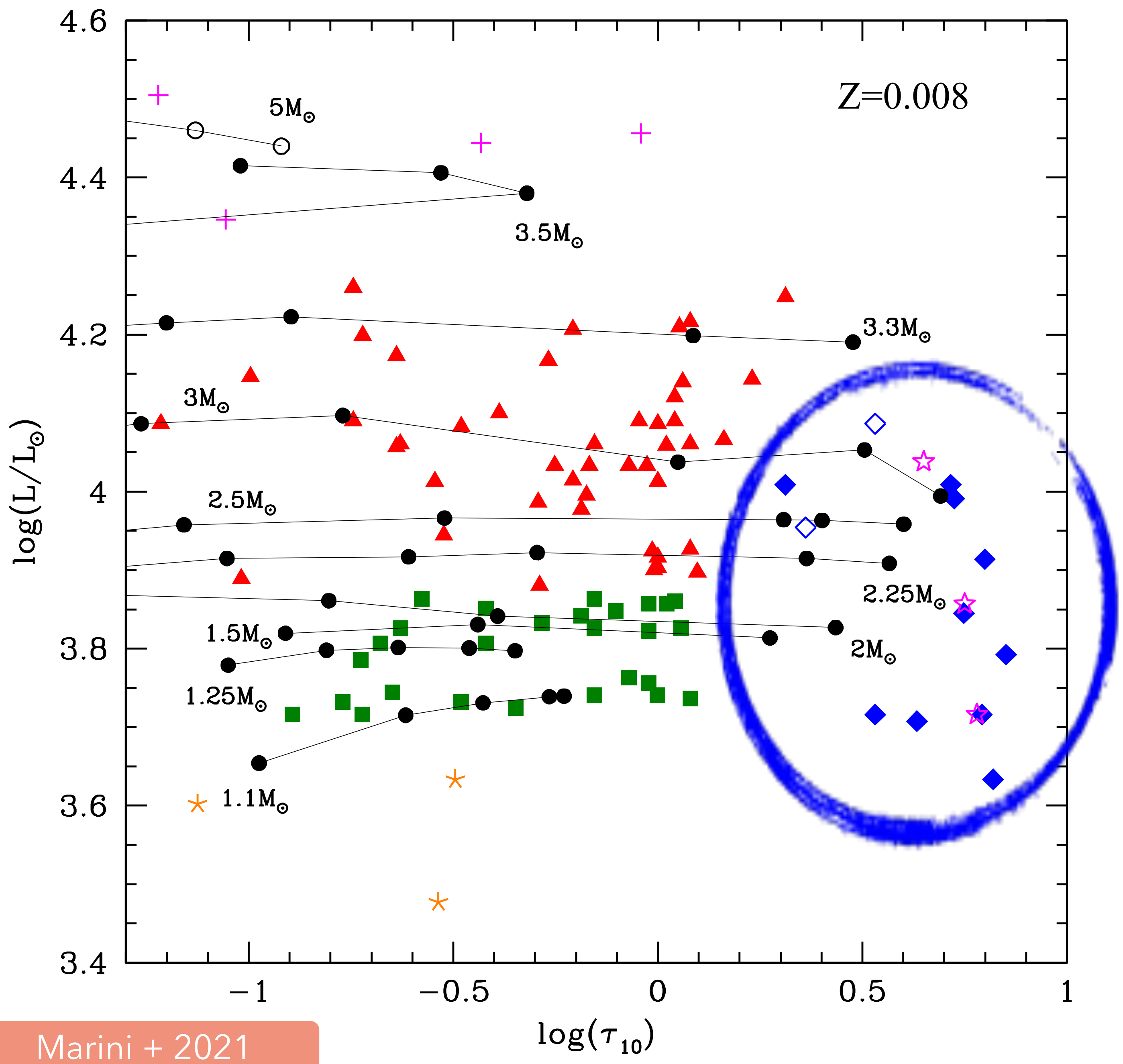
Z=0.008
5M⊙
3.5M⊙
3.3M⊙
3M⊙
2.5M⊙
2.25M⊙
2M⊙
1.5M⊙
1.25M⊙
1.1M⊙
log(L/L⊙)
log(τ10)
4.6
4.4
4.2
4
3.8
3.6
3.4
−1
−0.5
0
0.5
1

Marini + 2021

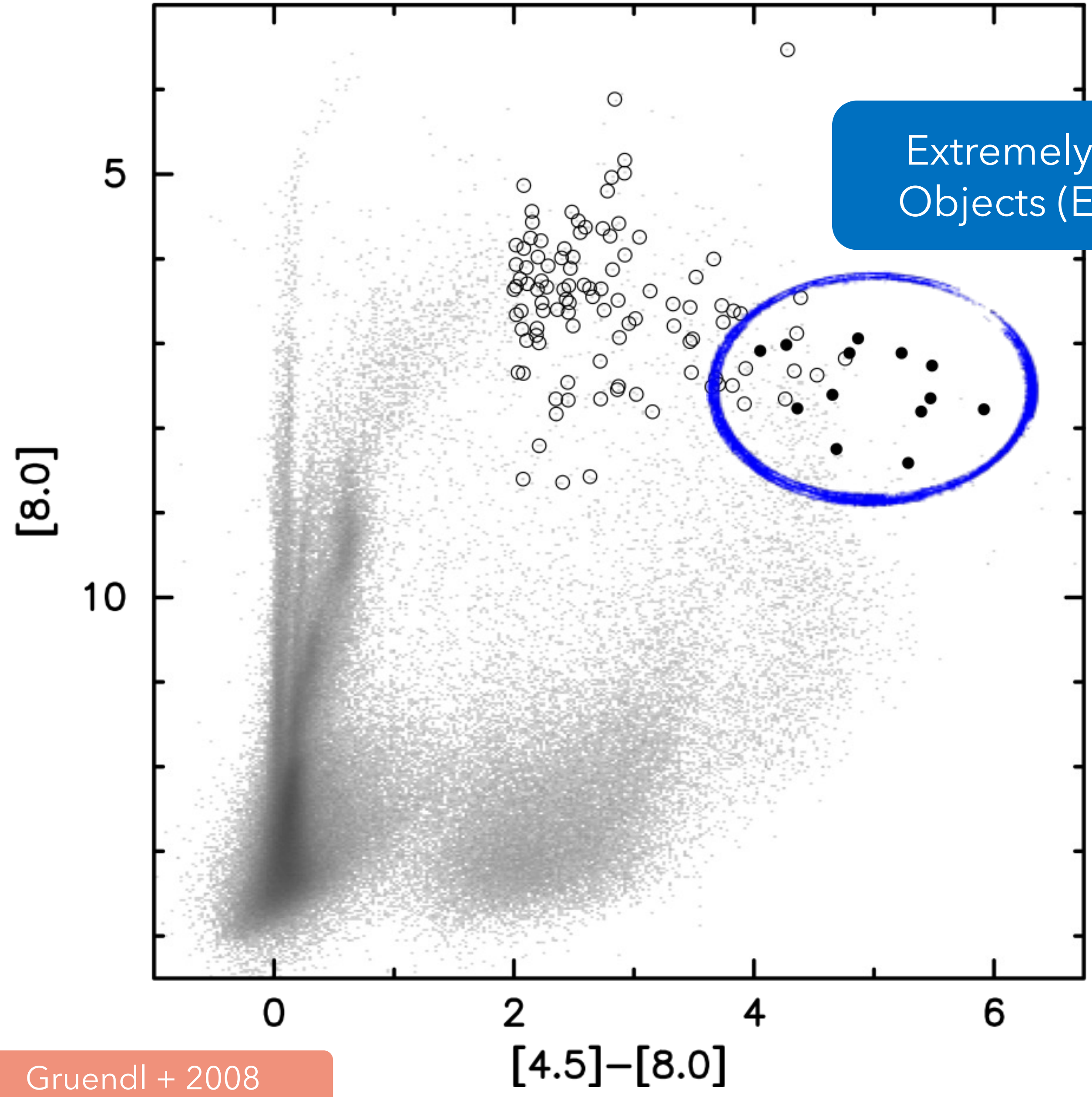

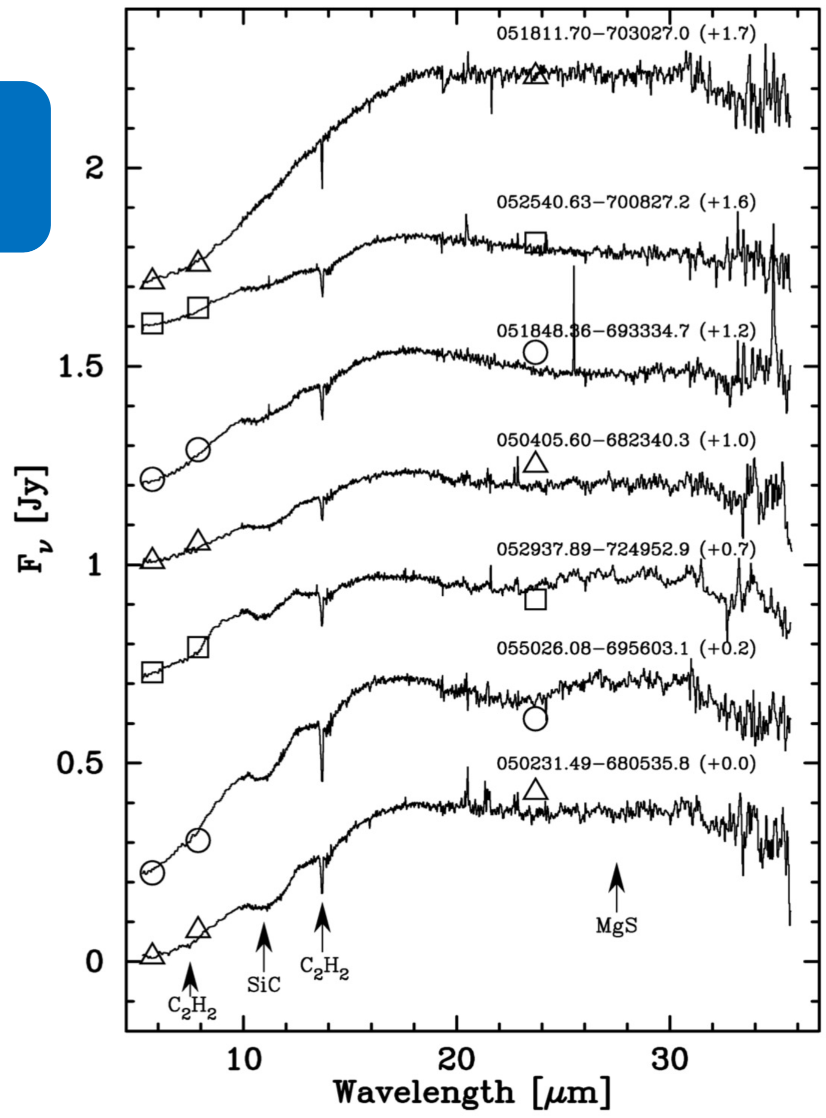

Gruendl + 2008

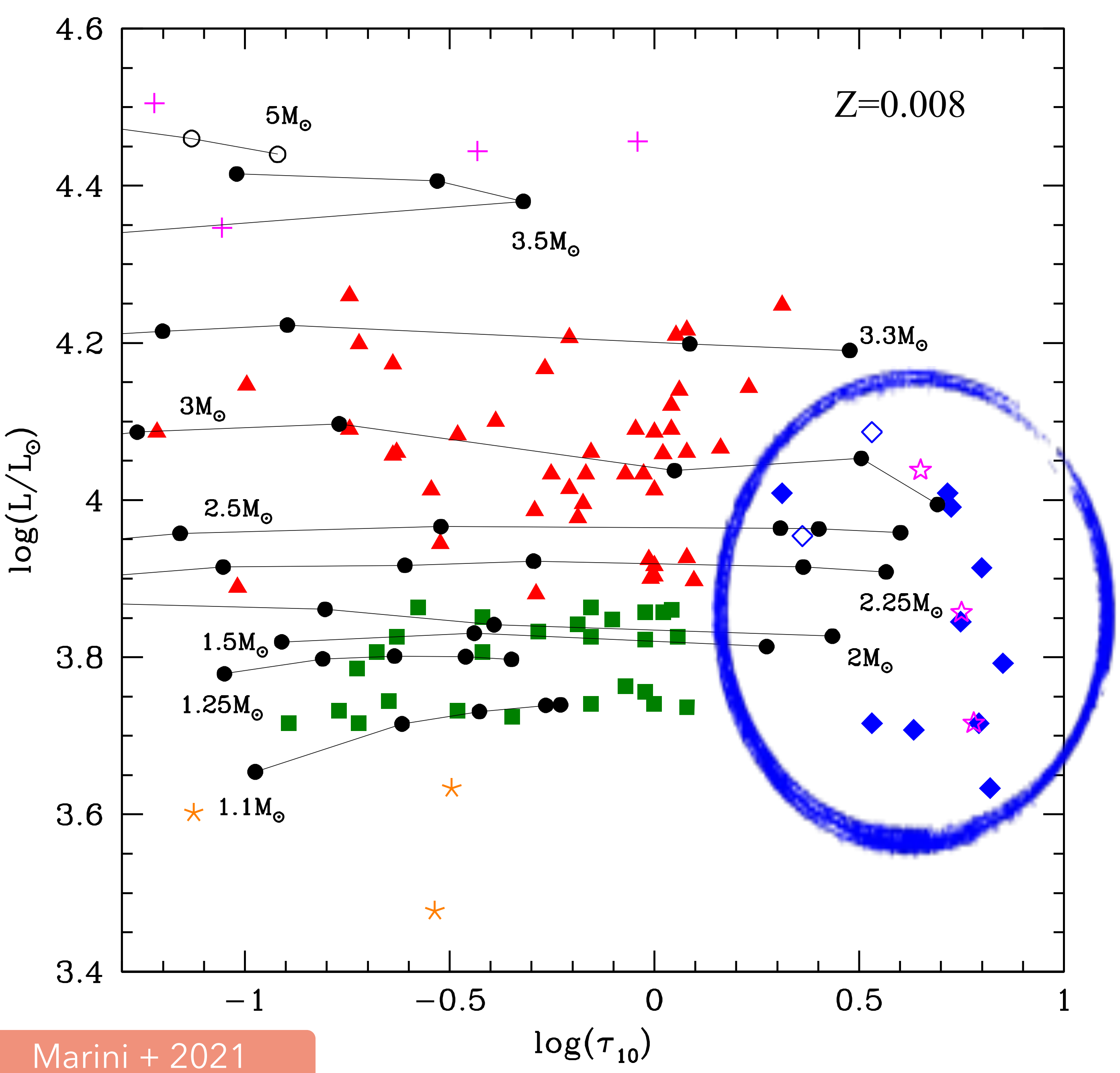

Z=0.008
5M⊙
3.5M⊙
3.3M⊙
3M⊙
2.5M⊙
2.25M⊙
2M⊙
1.5M⊙
1.25M⊙
1.1M⊙
log(L/L⊙)
log(τ10)
4.6
4.4
4.2
4
3.8
3.6
3.4
−1
−0.5
0
0.5
1

Marini + 2021

CASE C in Paczynski 1971, 1976

Image credits Lamers & Levesque, 2017

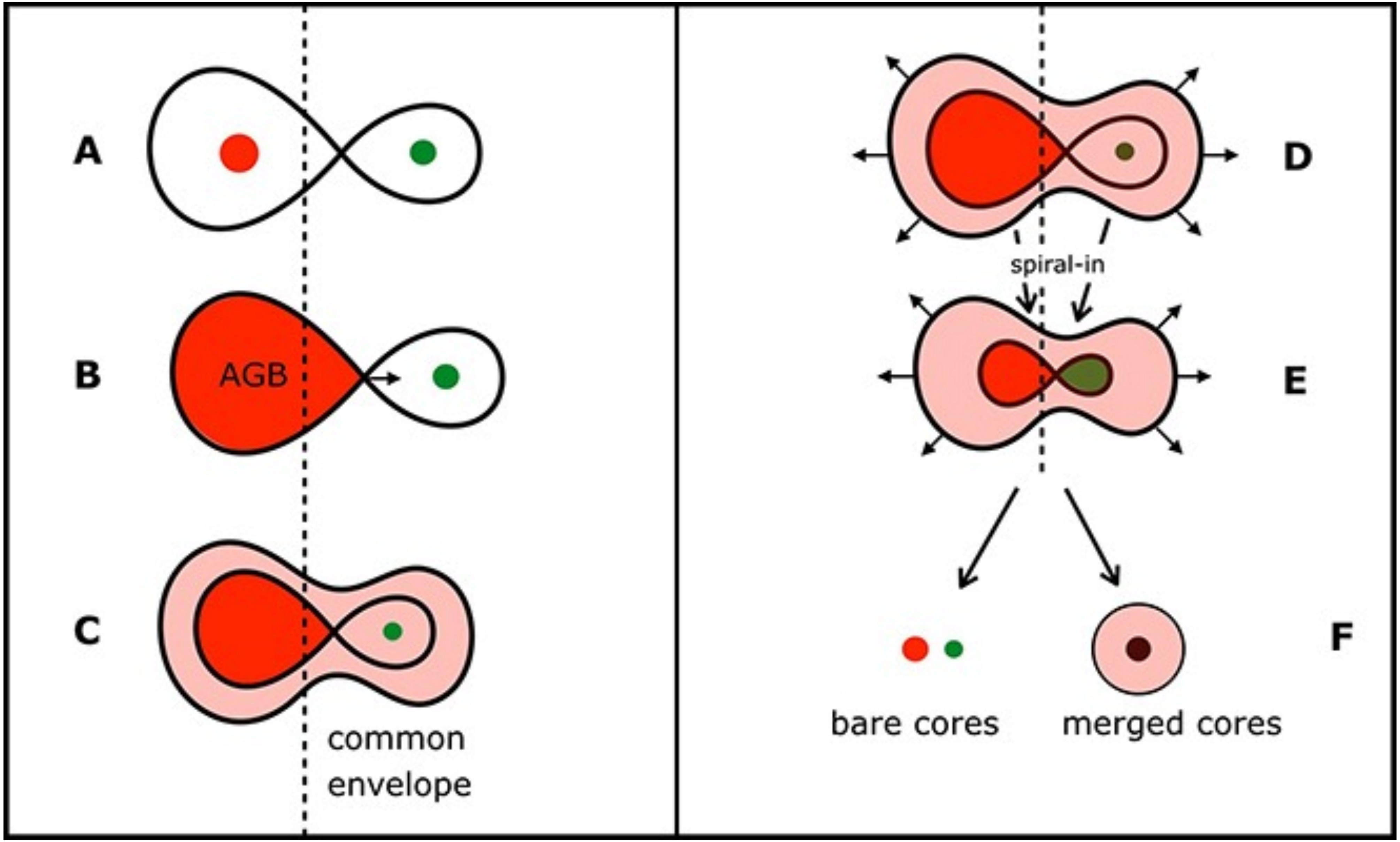

CASE C in Paczynski 1971, 1976

Image credits Lamers & Levesque, 2017

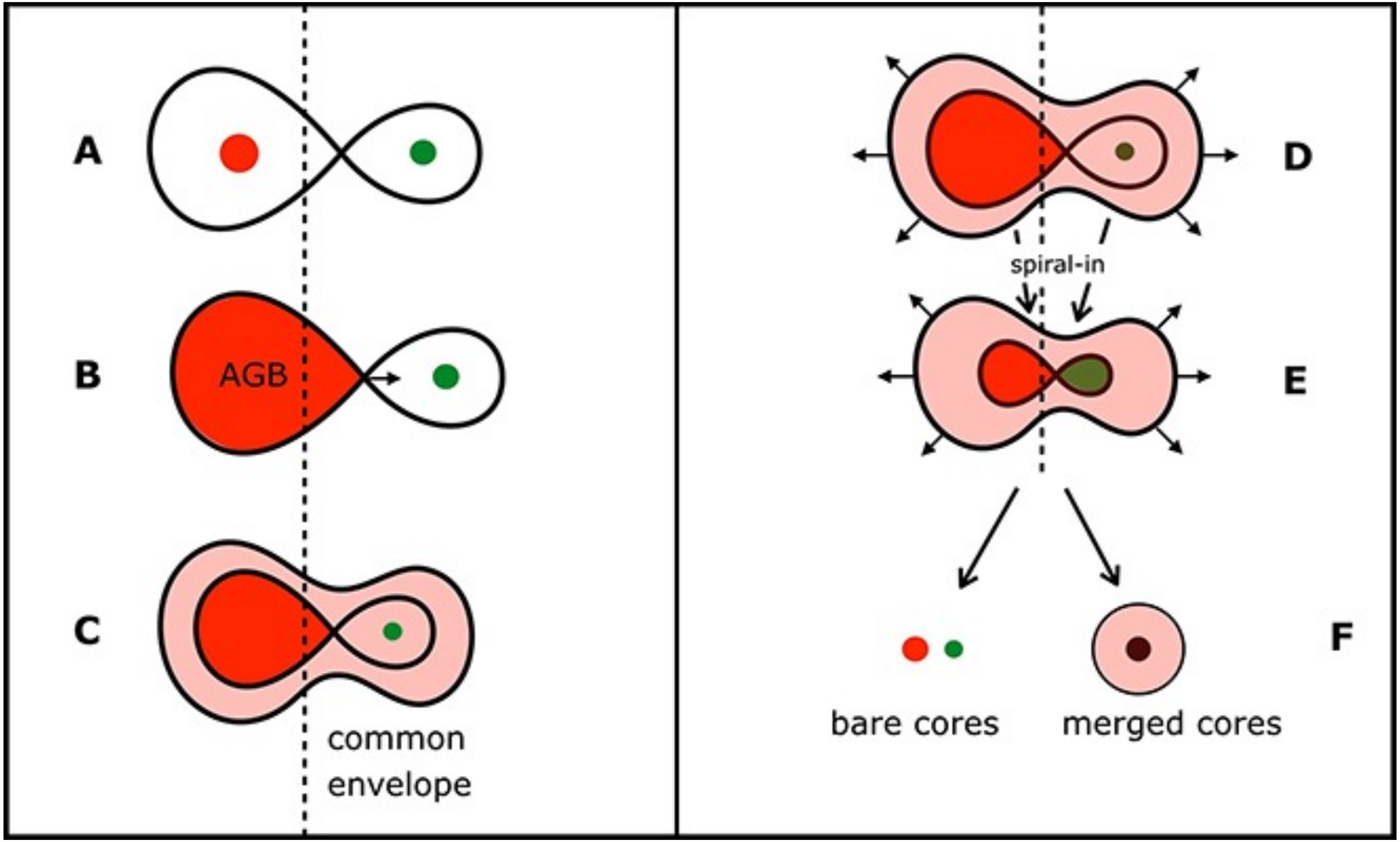

… an envelope of ~ 1 M⨀ can be lost even in 10 yr (Chamandy et al. 2020)

CASE C in Paczynski 1971, 1976

Image credits Lamers & Levesque, 2017

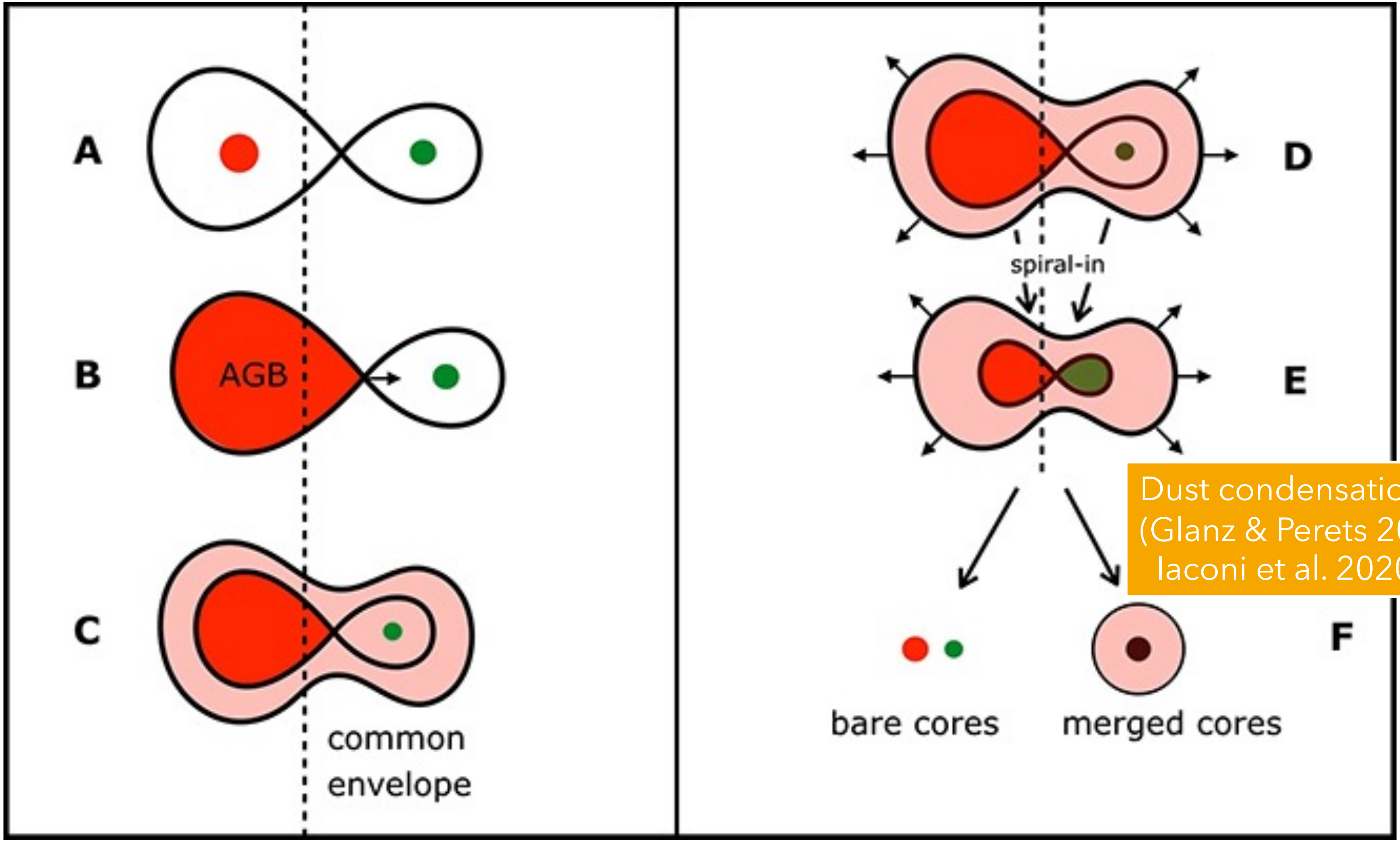

Dust condensation (Glanz & Perets 2018, Iaconi et al. 2020)

… an envelope of ~ 1 M⊙ can be lost even in 10 yr (Chamandy et al. 2020)

Monthly Notices
of the
ROYAL ASTRONOMICAL SOCIETY
MNRAS 502, L35–L39 (2021) doi:10.1093/mnrasl/slaa204

Are extreme asymptotic giant branch stars post-common envelope binaries?

F. Dell'Agli,[1★] E. Marini,[1,2] F. D'Antona,[1] P. Ventura,[1] M. A. T. Groenewegen,[3] L. Mattsson,[4] D. Kamath,[5] D. A. García-Hernández[6,7] and M. Tailo[8]

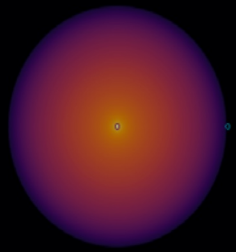

Which are the evolutionary boundaries for which systems evolve into stable case C evolution is feasible?
How much dust can be formed in this condition?

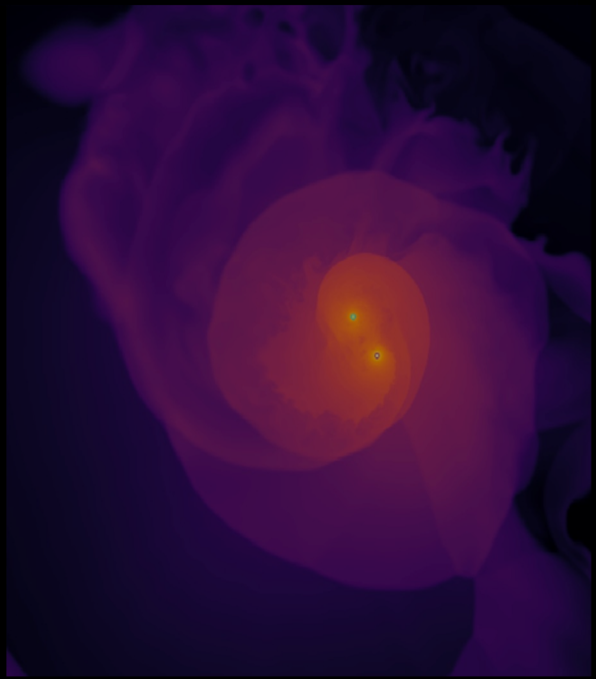

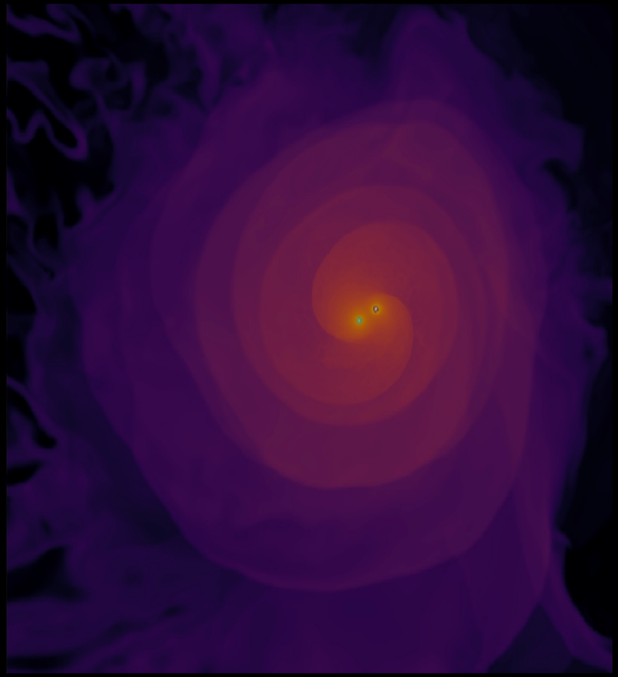

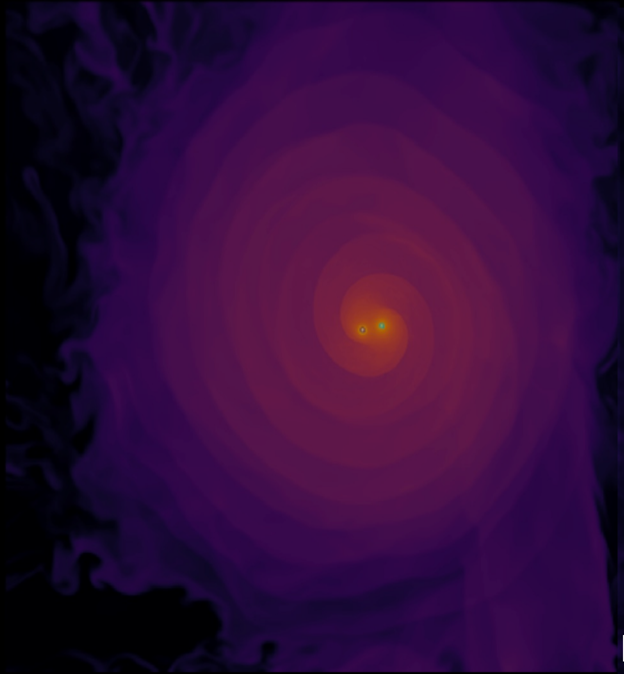

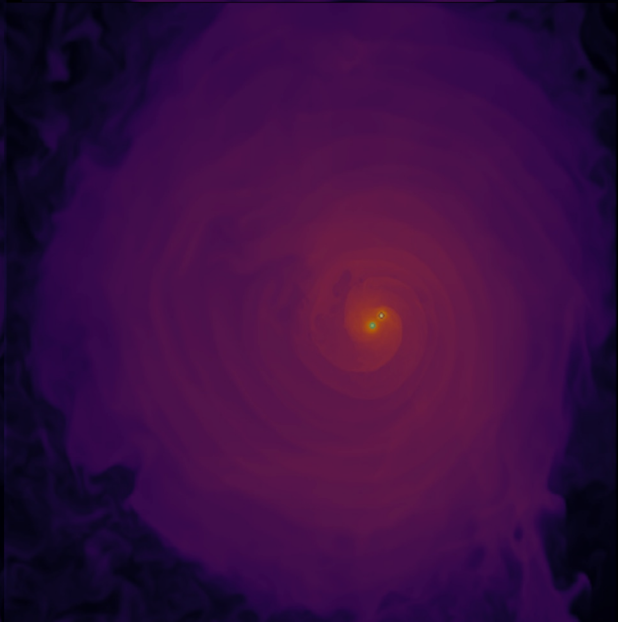

Image credits Chamandy+2020

Monthly Notices of the ROYAL ASTRONOMICAL SOCIETY
MNRAS 502, L35–L39 (2021) doi:10.1093/mnrasl/slaa204

Are extreme asymptotic giant branch stars post-common envelope binaries?

F. Dell'Agli [1★], E. Marini [1,2] F. D'Antona [1] P. Ventura [1] M. A. T. Groenewegen [3] L. Mattsson [4] D. Kamath [5] D. A. García-Hernández [6,7] and M. Tailo [8]

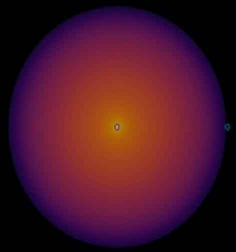

Which are the evolutionary boundaries for which systems evolve into stable case C evolution is feasible? How much dust can be formed in this condition?

We looked at those systems which:

I. suffer unavoidable CE evolution
II. when they are already carbon stars
III. where the CE allows to meet the required dust density production which is not allowed during the single stellar evolution.

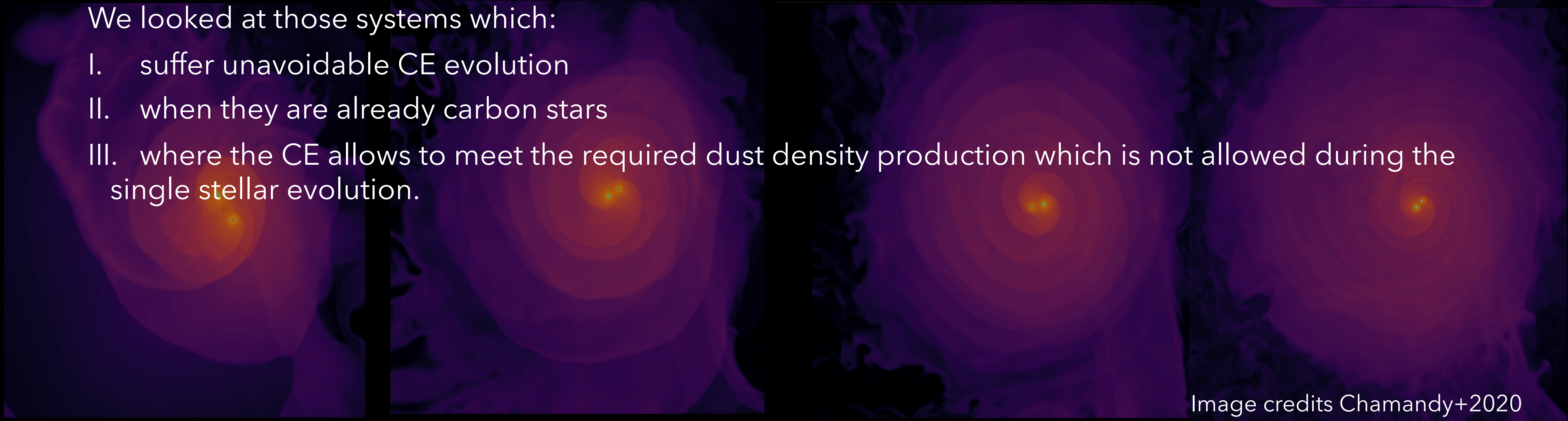

Image credits Chamandy+2020

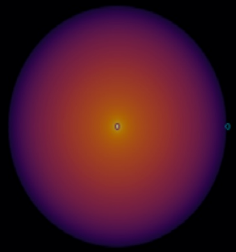

Monthly Notices of the ROYAL ASTRONOMICAL SOCIETY
MNRAS **502,** L35–L39 (2021) doi:10.1093/mnrasl/slaa204

Are extreme asymptotic giant branch stars post-common envelope binaries?

F. Dell'Agli,[1★] E. Marini,[1,2] F. D'Antona,[1] P. Ventura,[1] M. A. T. Groenewegen,[3] L. Mattsson,[4] D. Kamath,[5] D. A. García-Hernández[6,7] and M. Tailo[8]

Which are the evolutionary boundaries for which systems evolve into stable case C evolution is feasible? How much dust can be formed in this condition?

We looked at those systems which:

I. suffer unavoidable CE evolution
II. when they are already carbon stars
III. where the CE allows to meet the required dust density production which is not allowed during the single stellar evolution.

We assume:

- a system of M1=1.1, 2.5, 3.0 Msun with a companion M2=0.6, 0.8 Msun
- a mass loss rate of 5x10^-4 Msun/yr

Image credits Chamandy+2020

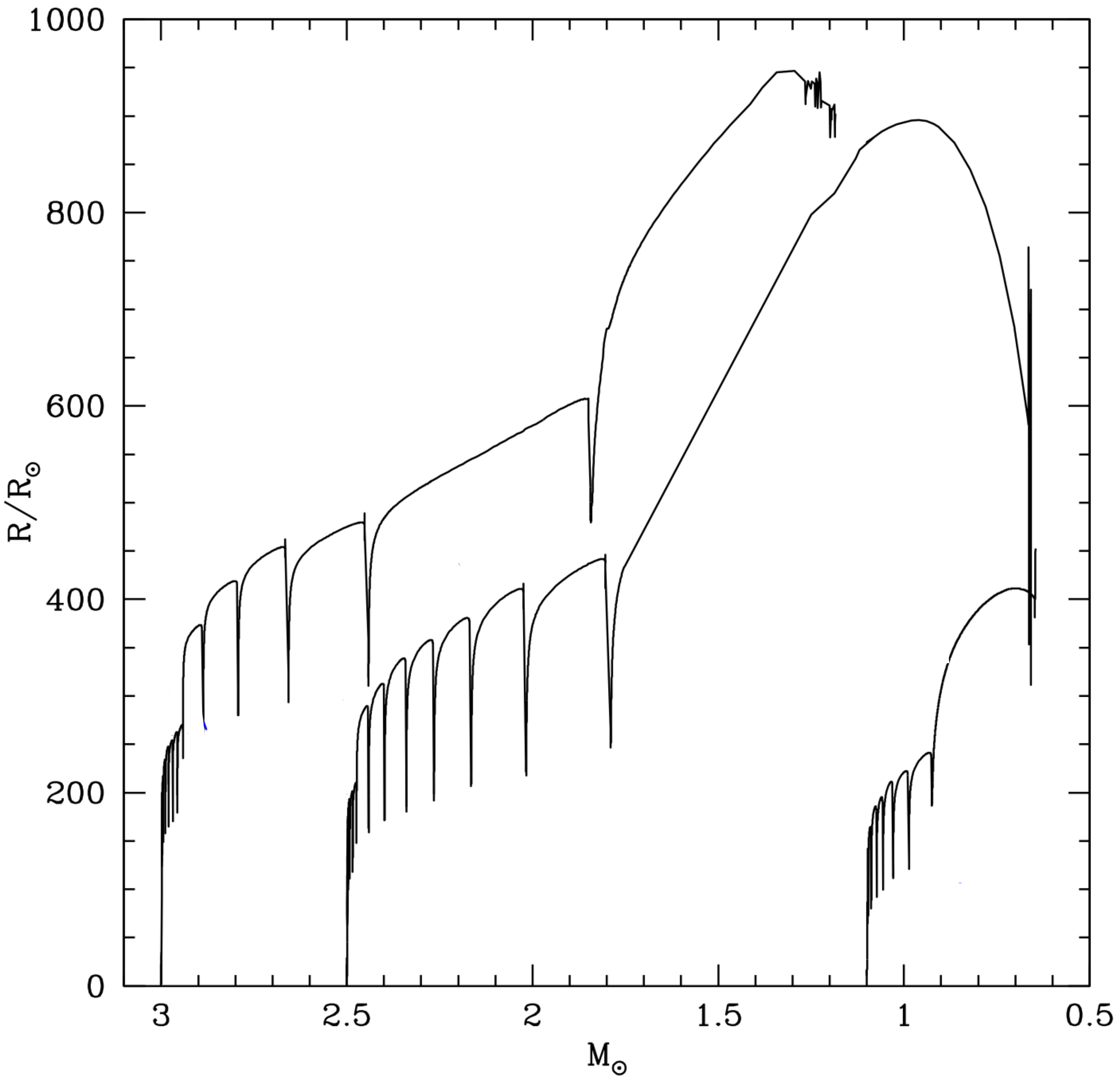

Dell'Agli+2021

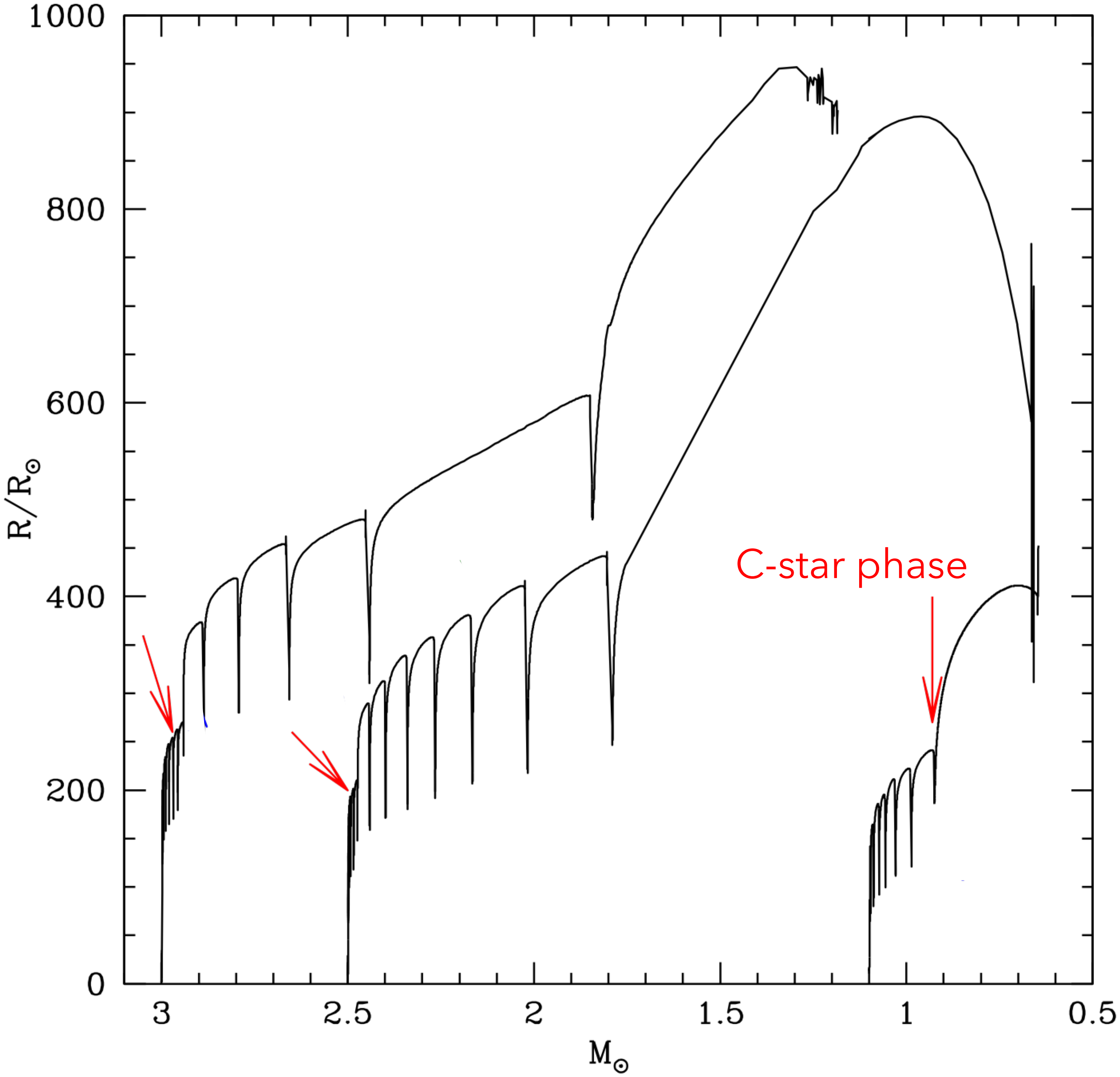

Dell'Agli+2021

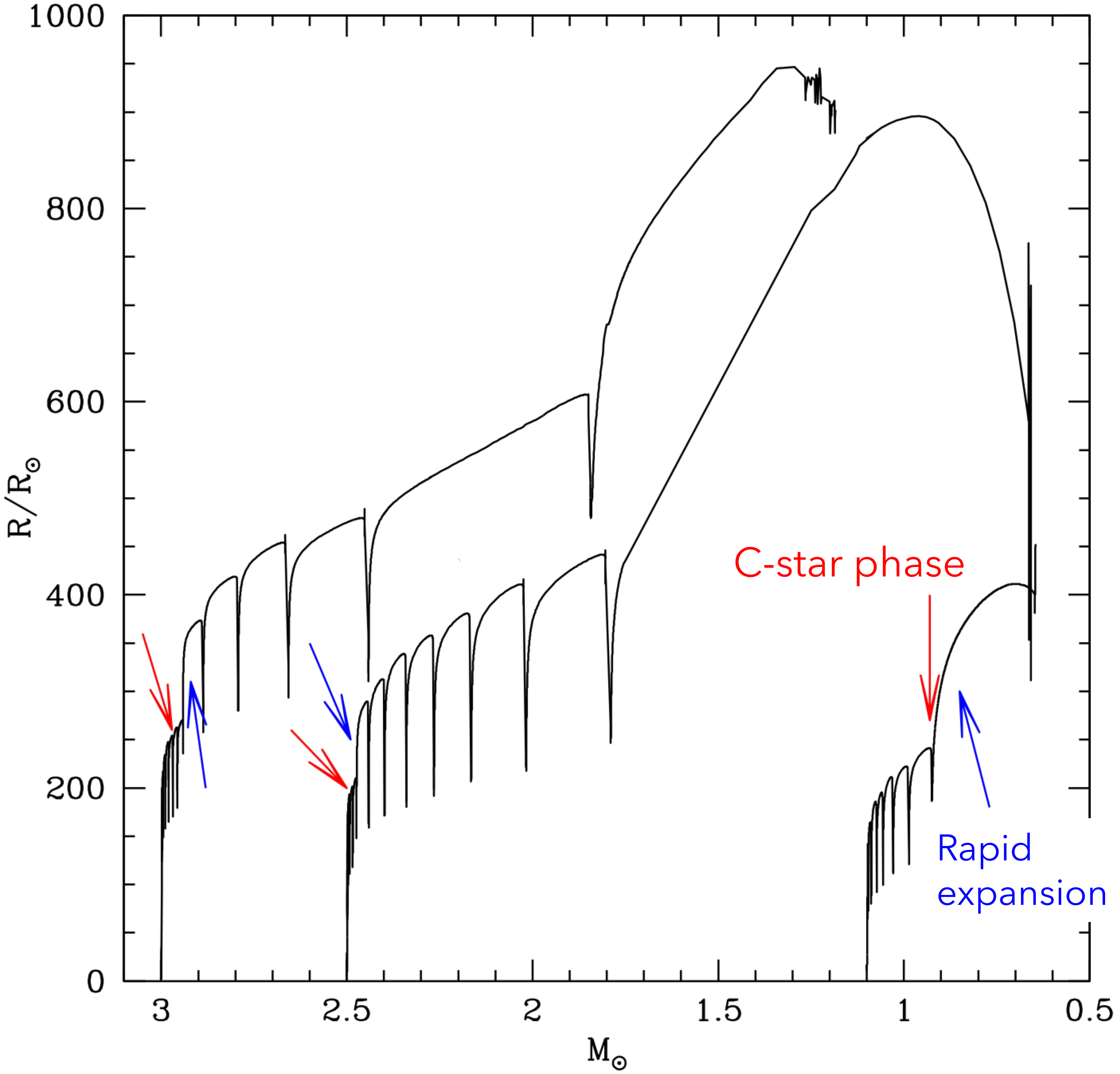

Dell'Agli+2021

The initial period of a binary in which the AGB fills the Roche-Lobe at each point of mass along its single stellar evolution

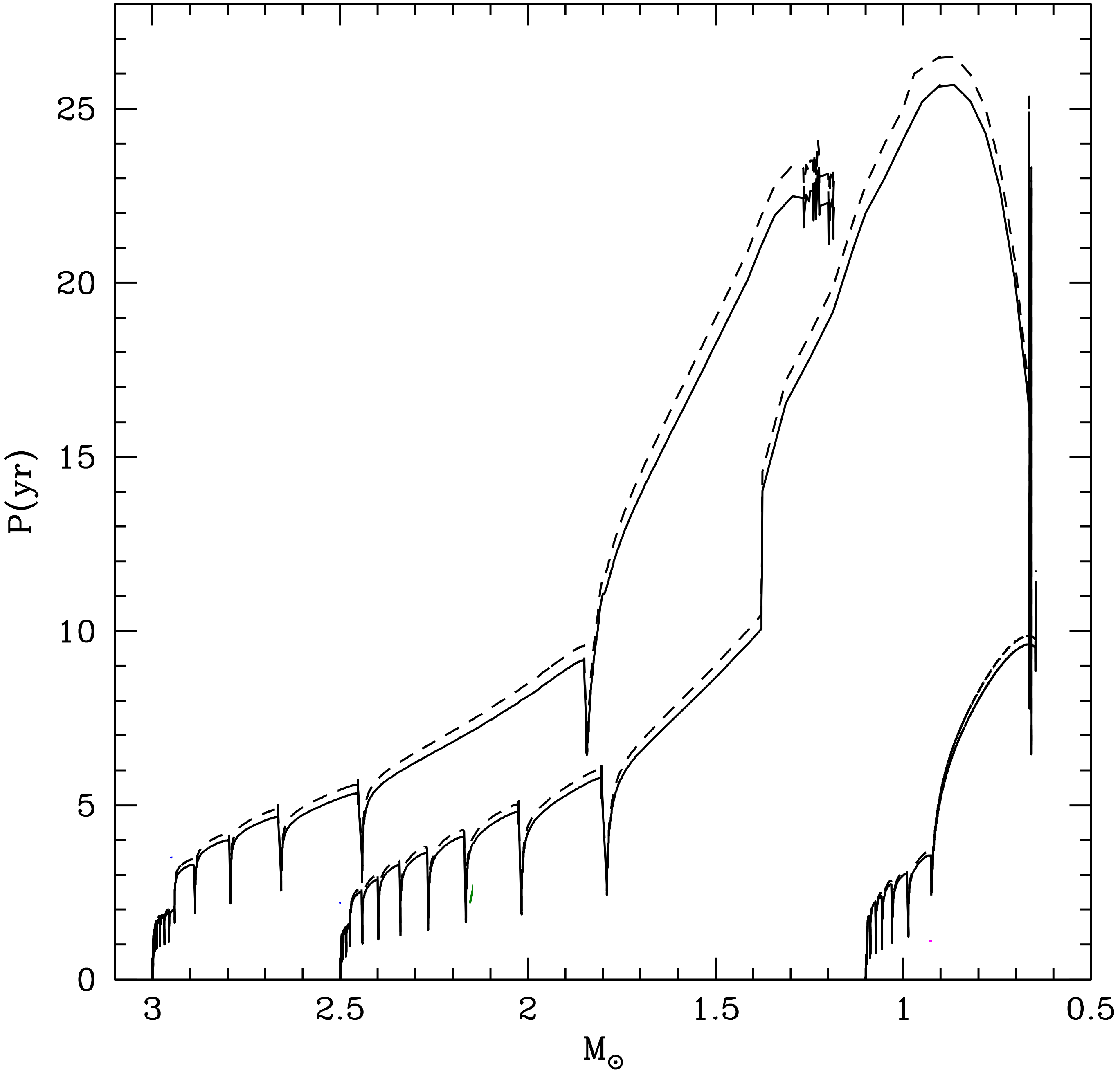

Dell'Agli+2021

The initial period of a binary in which the AGB fills the Roche-Lobe at each point of mass along its single stellar evolution

Wide range of initial periods ~ 2.5-15 yrs during which this may happen

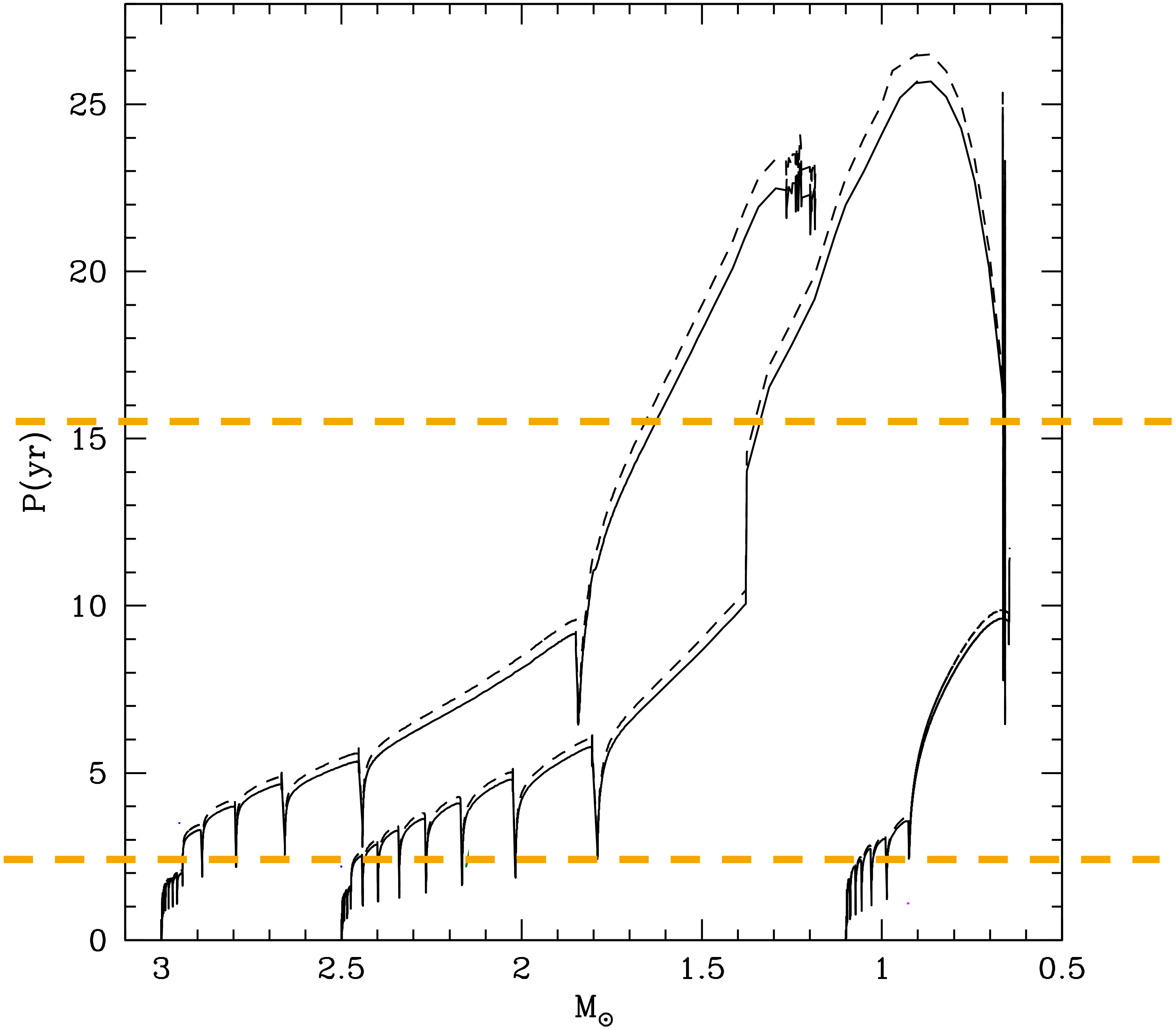

Dell'Agli+2021

The initial period of a binary in which the AGB fills the Roche-Lobe at each point of mass along its single stellar evolution

Wide range of initial periods ~ 2.5-15 yrs during which this may happen

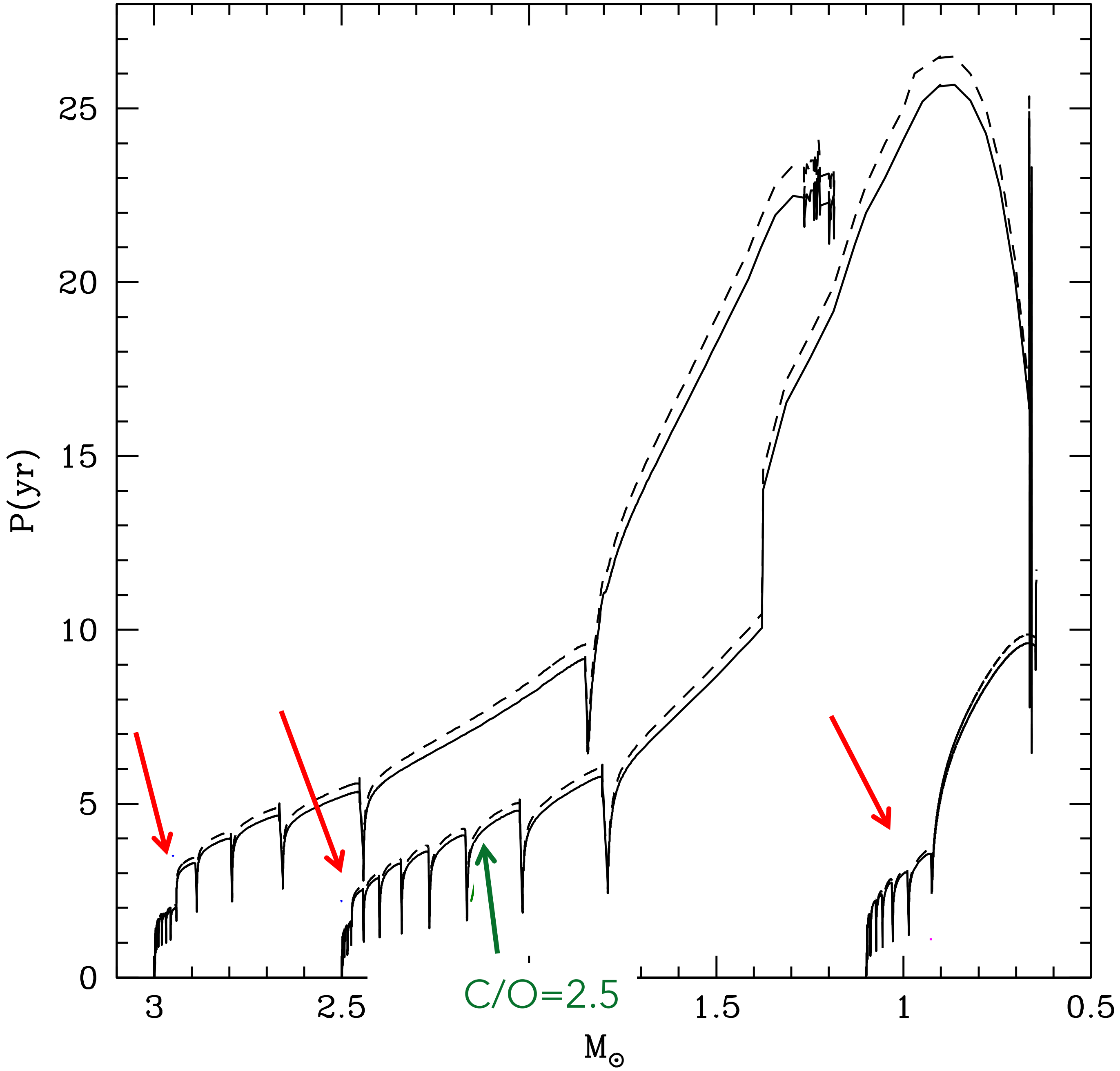

Dell'Agli+2021

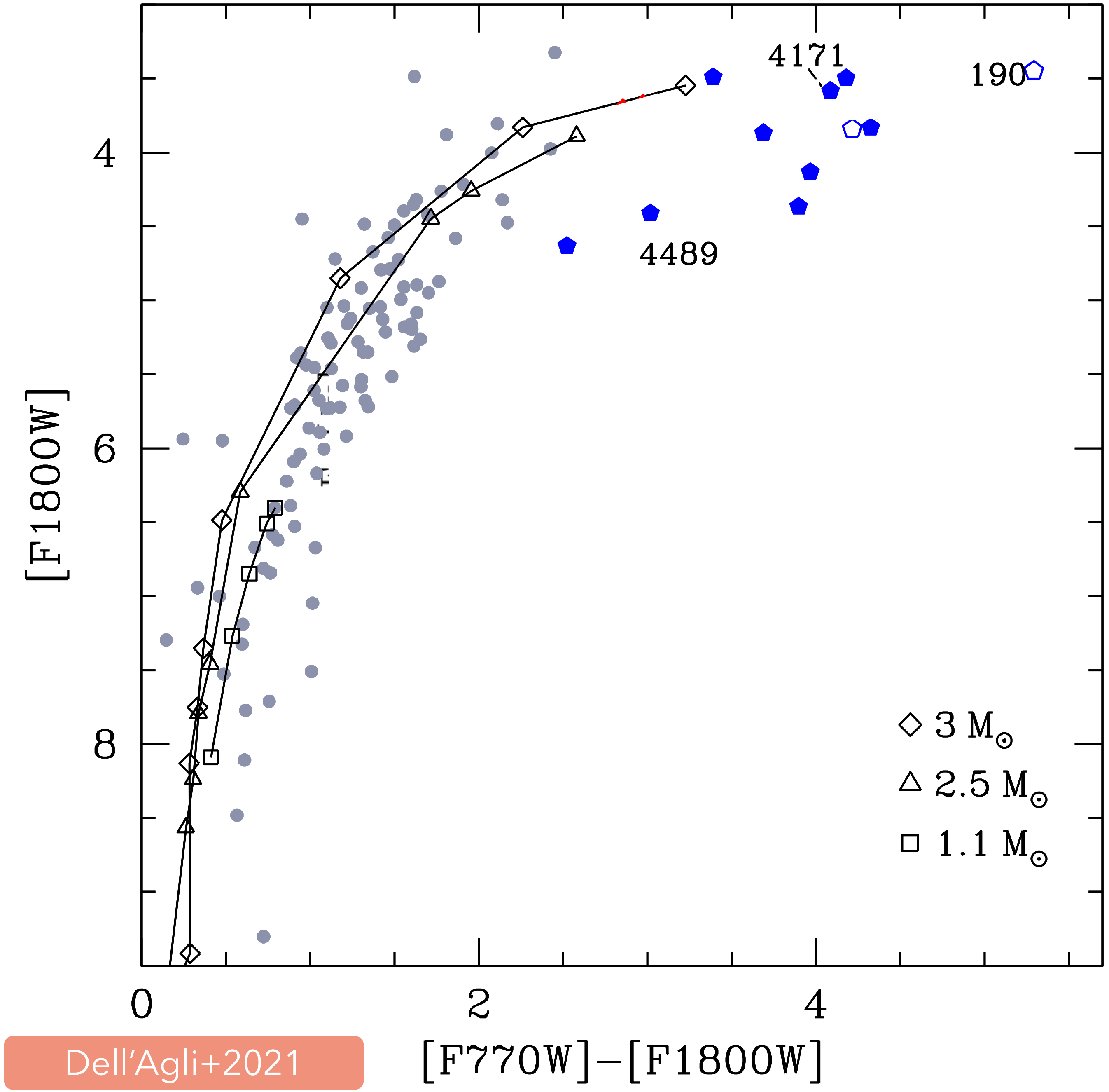

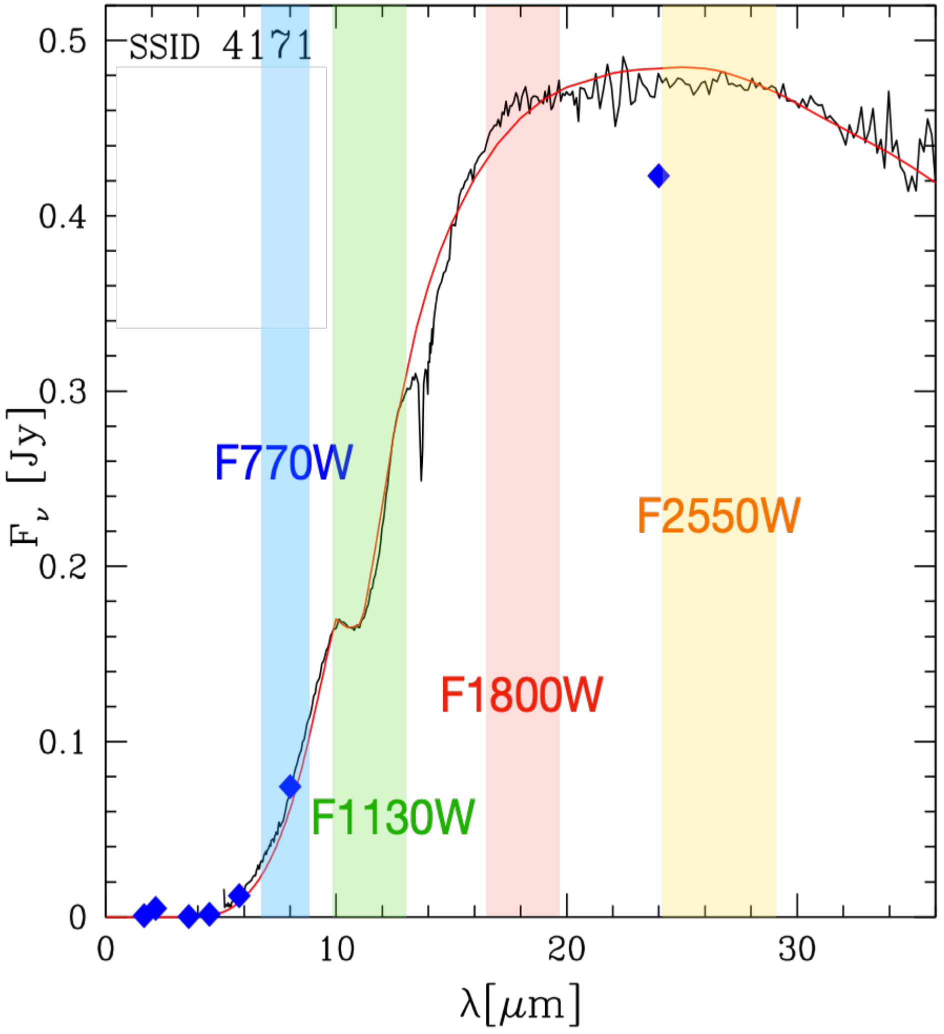

Dell'Agli+2021

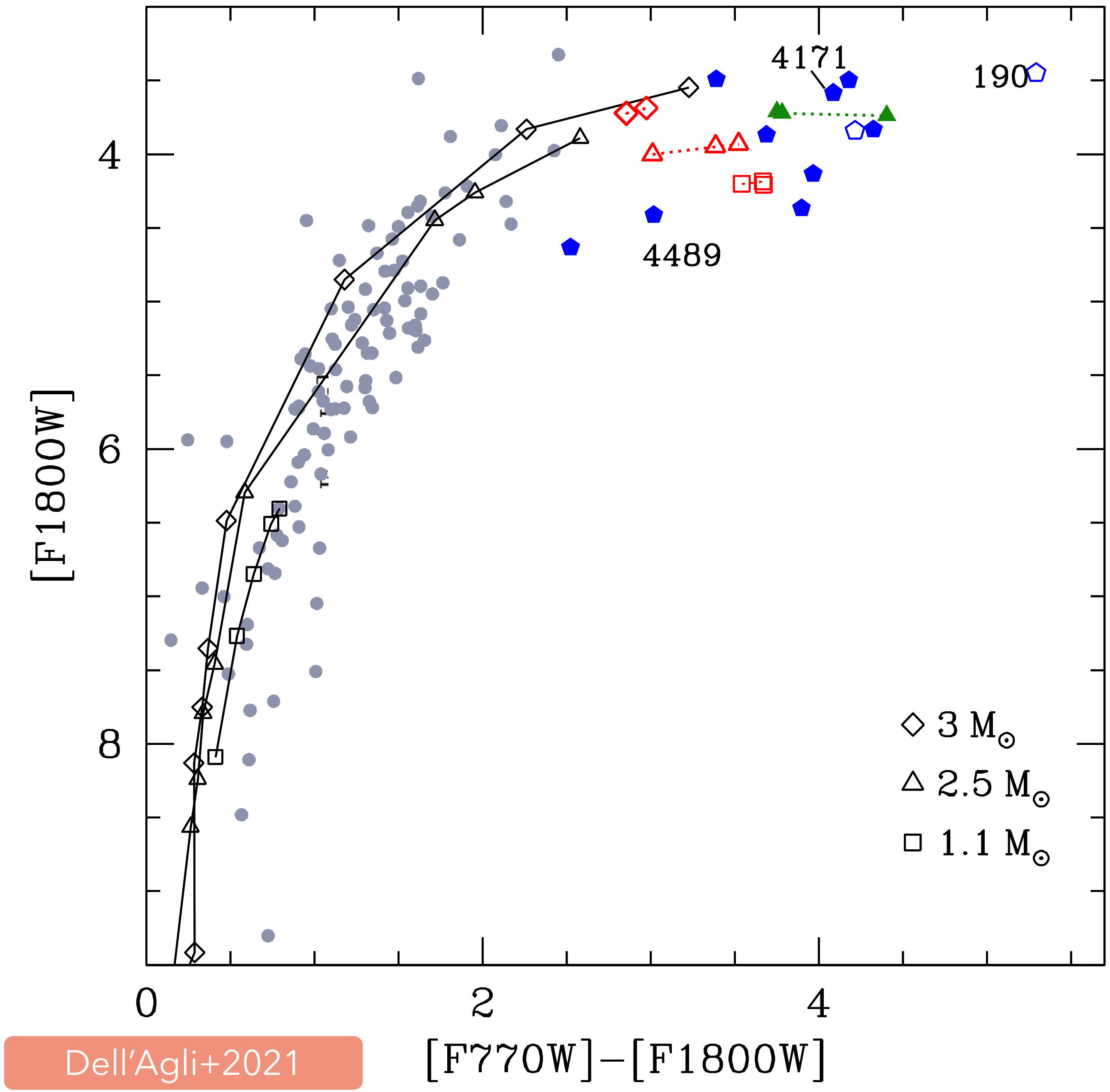

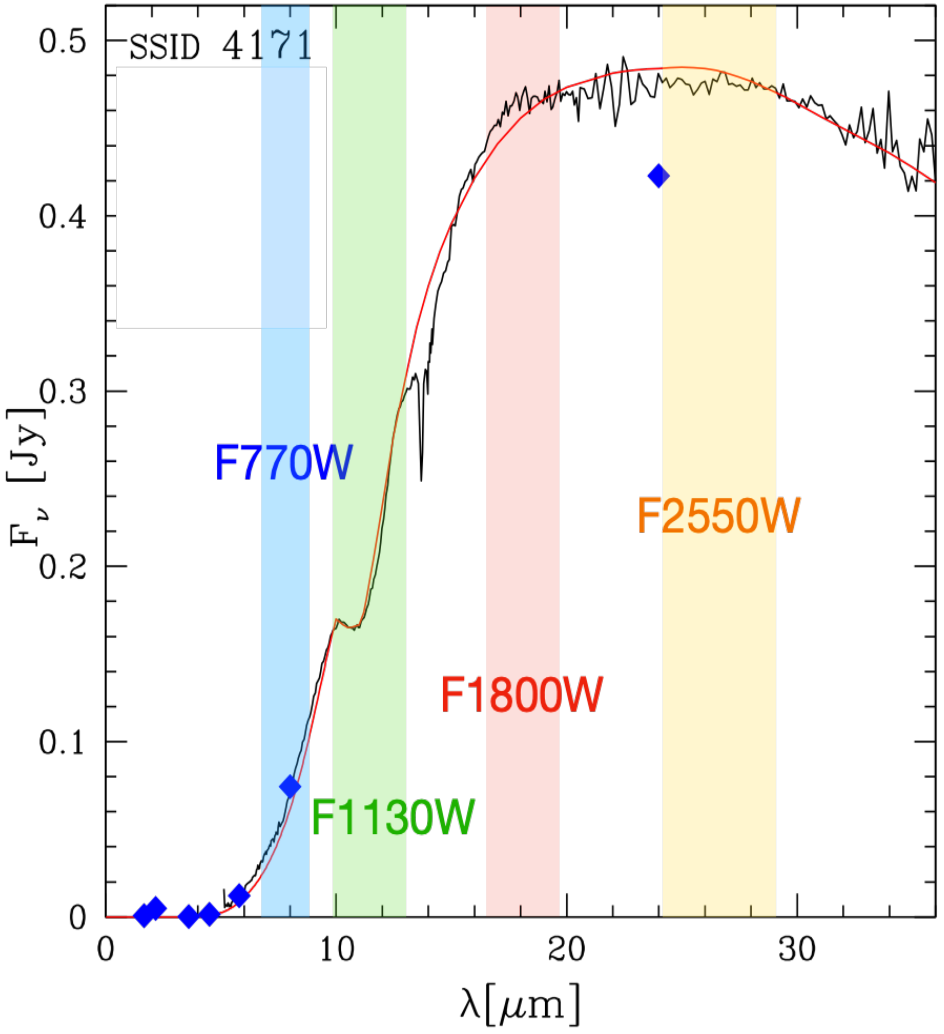

Dell'Agli+2021

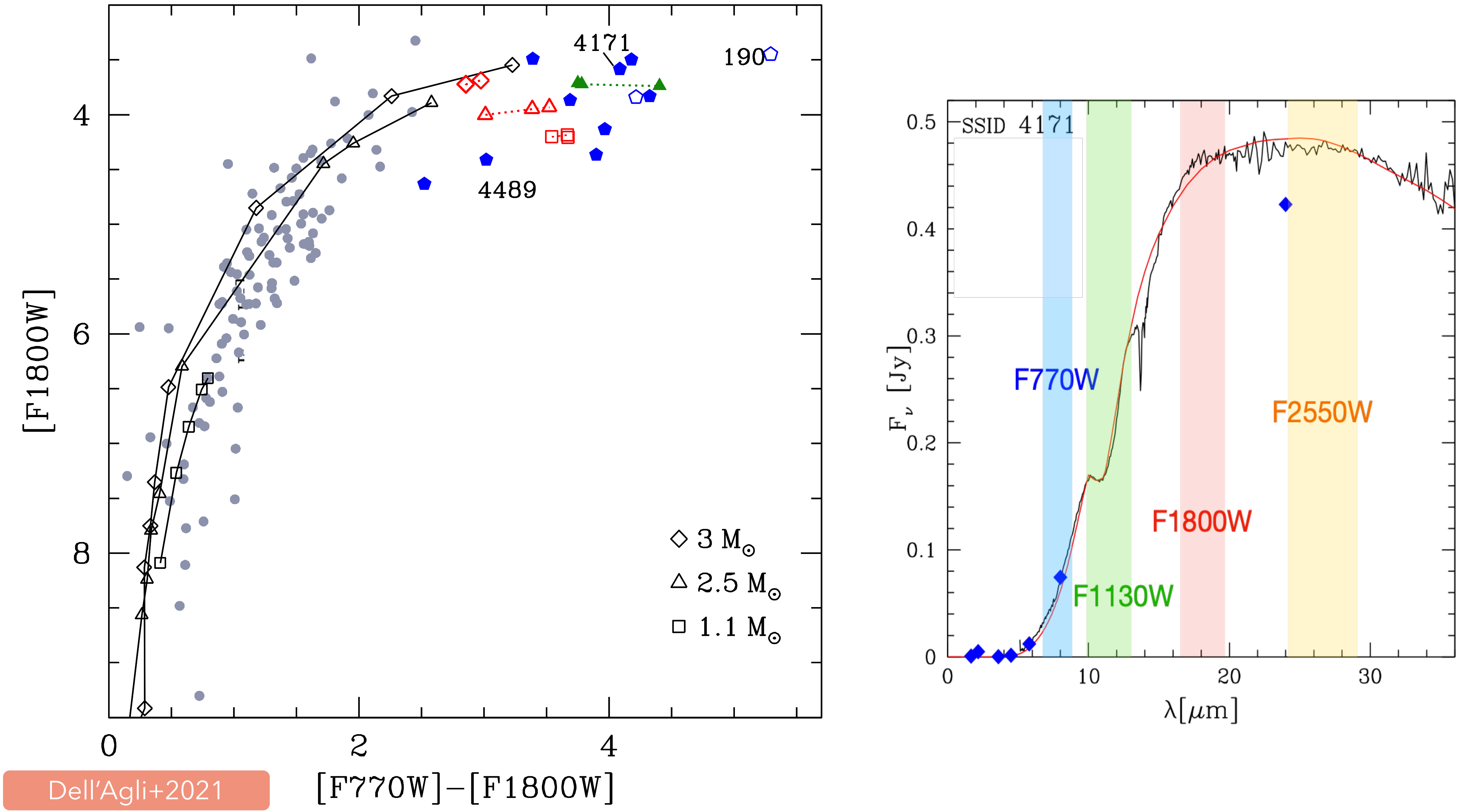

Dell'Agli+2021

CONCLUSIONS

EROs could be interpreted as:

- the result of the evolution of binaries of periods ~2.5–15 yrs
- the primary: an AGB star of mass 1.1–3.0 M evolving through the C-star phase
- the companion: a star of mass low enough that the mass transfer is unstable.

More observational constrains are needed (see e.g.Sloan et al. 2016, Groenewegen 2021)

TAKE HOME MESSAGE

Proof of concept for the hypothesis that the parameters of the CE evolution are not particularly tight and that the resulting dust is indeed of a density high enough to produce the colours of the EROs.

Image credits Chamandy+2020

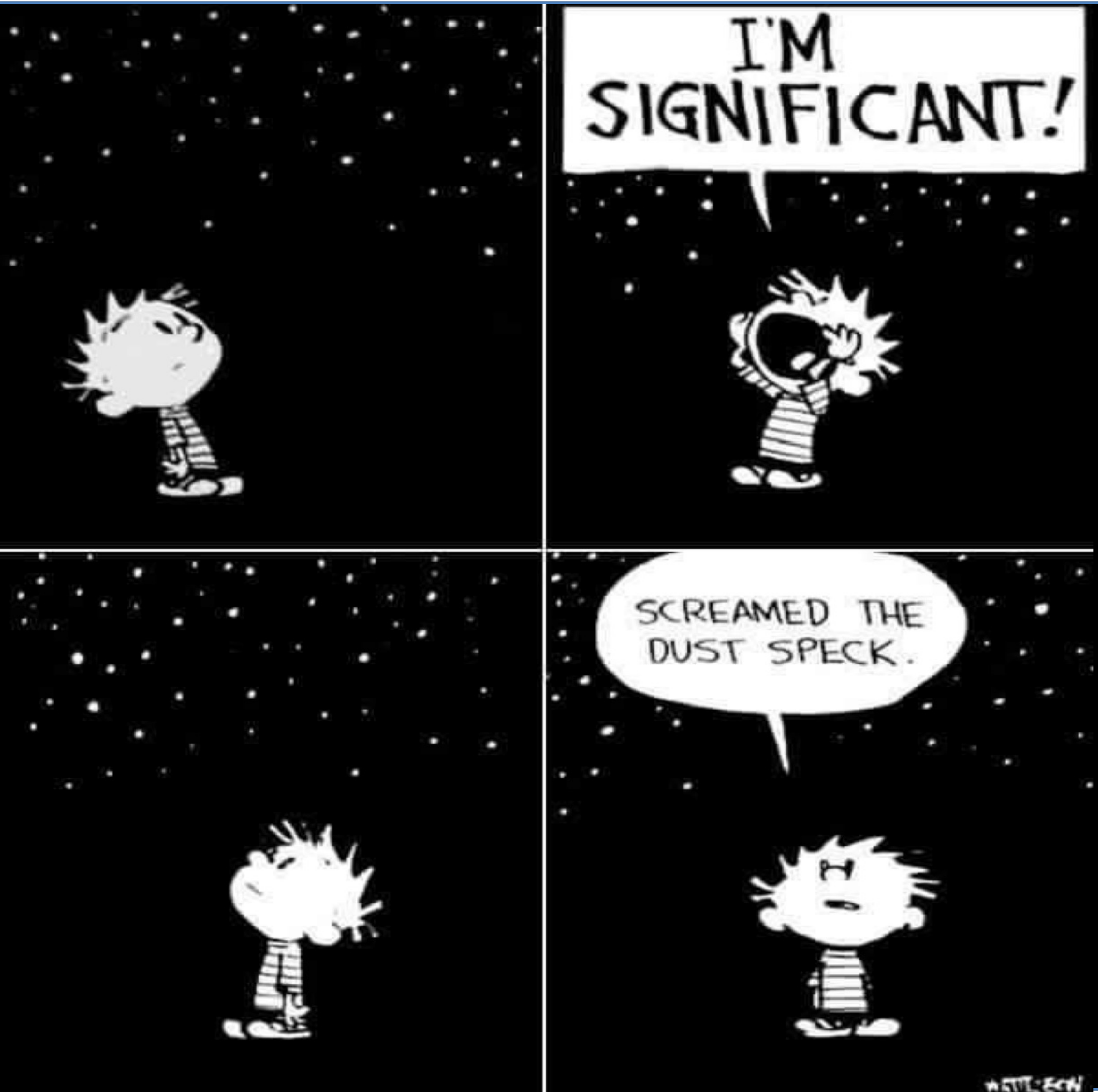

Thank you!

Marini et al. 2021

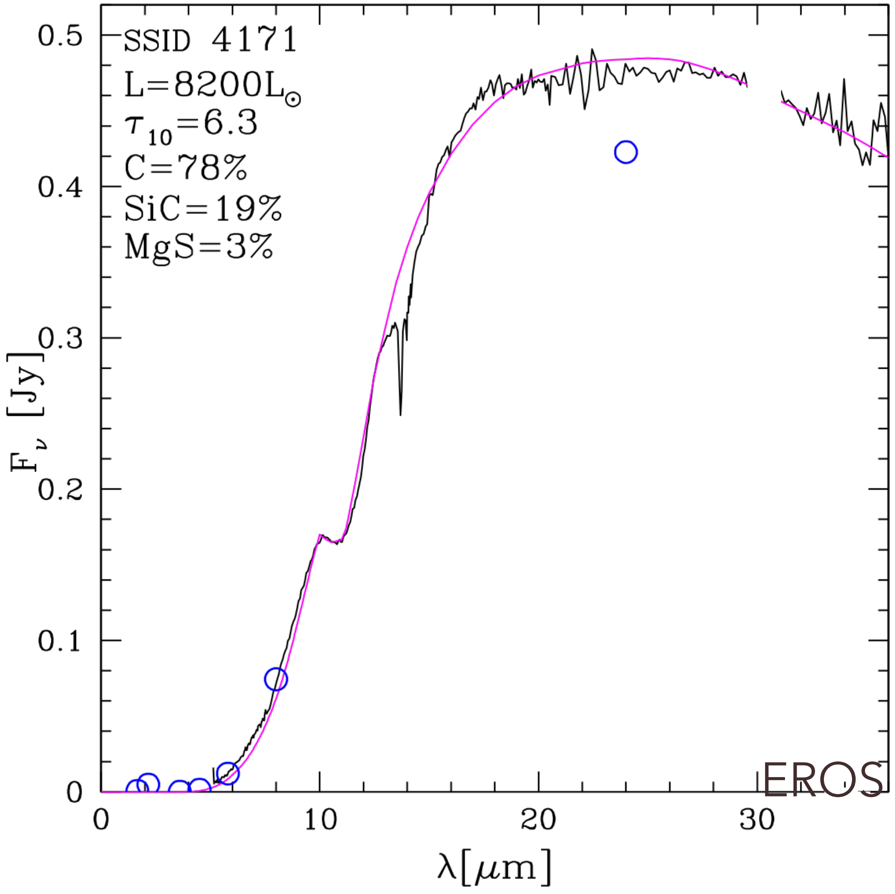

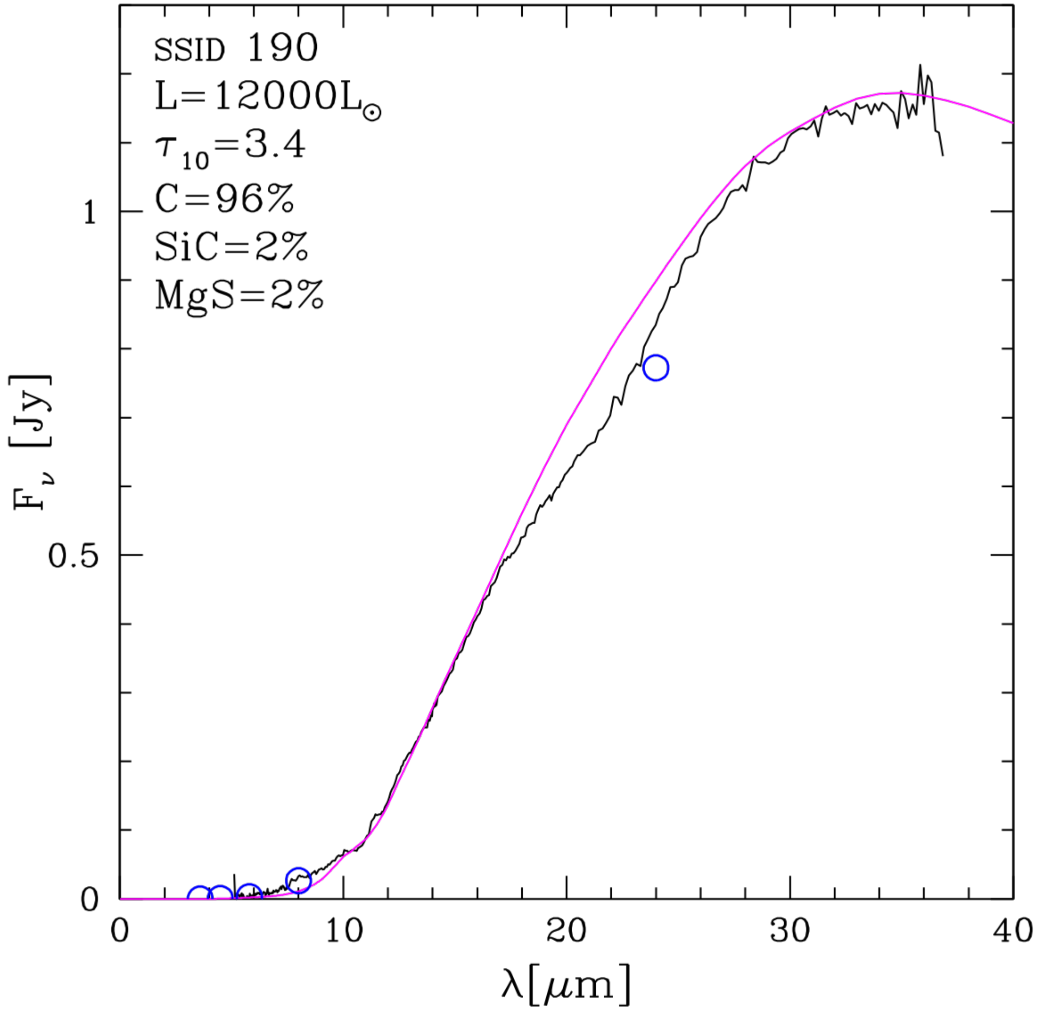

Table 1. Summary of the interpretation of the stars discussed in this work: *Spitzer* and IRAC/ERO name, coordinates, luminosity, optical depth, percentages of the different dust species (in order: solid carbon, silicon carbide, magnesium sulphide, graphite), initial mass and age.

SSID	IRAS/ERO name	RA (deg)	Dec. (deg)	$L/L_\odot$	τ_{10}	%(C)	%(SiC)	%(MgS)	%(graph)	$M_{init}/M_\odot$	Age (Gyr)
4185	IRAS 05042–6827	76.0233	−68.3945	5200	6.2	67	25	2	6	1.1−1.2	5.0−7.0
4299	IRAS 05187–7033	79.5488	−70.5075	9800	5.3	79	0	0	21	2.5−3.0	0.4−0.6
4308	IRAS 05191–6936	79.7016	−69.5596	7000	5.6	64	22	2	12	2.0−2.5	0.6−1.0
4415	IRAS 05260–7010	81.4193	−70.1409	4700	6.6	68	18	2	12	1.1−1.2	5.0−7.0
4171	ERO 0502315	75.6312	−68.0934	8200	6.3	68	19	3	10	2.0−2.5	0.6−1.0
4489	IRAS 05305–7251	82.4079	−72.8314	5100	4.3	53	40	3	4	1.1−1.2	5.0−7.0
4781	IRAS 05509–6956	87.6091	−69.9342	10 200	5.2	68	27	3	2	2.5−3.0	0.4−0.6
9	IRAS 04518–6852	72.9192	−68.7930	5200	3.4	75	14	5	6	1.1−1.2	5.0−7.0
65	IRAS 05133–6937	78.2576	−69.5642	6200	7.1	76	20	2	2	1.5−2.0	1.0−2.0
125	IRAS 05315–7145	82.6853	−71.7167	9000	2.3	62	14	2	24	2.0−2.5	0.6−1.0
190	IRAS 05495–7034	87.2504	−70.5562	12 200	3.4	83	2	2	15	3.0−3.5	0.3−0.4